BAMS Article

A Primer on Phased Array Radar Technology for the Atmospheric Sciences

Robert Palmer, David Bodine, Pavlos Kollias, David Schvartzman, Dusan Zrnić, Pierre Kirstetter, Guifu Zhang, Tian-You Yu, Matthew Kumjian, Boonleng Cheong, Scott Collis, Stephen Frasier, Caleb Fulton, Kurt Hondl, James Kurdzo, Tomoo Ushio, Angela Rowe, Jorge Salazar-Cerreño, Sebastián Torres, Mark Weber, and Mark Yeary

ABSTRACT: The scientific community has expressed interest in the potential of phased array radars (PARs) to observe the atmosphere with finer spatial and temporal scales. Although convergence has occurred between the meteorological and engineering communities, the need exists to increase access of PAR to meteorologists. Here, we facilitate these interdisciplinary efforts in the field of ground-based PARs for atmospheric studies. We cover high-level technical concepts and terminology for PARs as applied to studies of the atmosphere. A historical perspective is provided as context along with an overview of PAR system architectures, technical challenges, and opportunities. Envisioned scan strategies are summarized because they are distinct from traditional mechanically scanned radars and are the most advantageous for high-resolution studies of the atmosphere. Open access to PAR data is emphasized as a mechanism to educate the future generation of atmospheric scientists. Finally, a vision for the future of operational networks, research facilities, and expansion into complementary radar wavelengths is provided.

KEYWORDS: Atmosphere; Instrumentation/sensors; Radars/Radar observations

https://doi.org/10.1175/BAMS-D-21-0172.1
Corresponding author: Robert Palmer, rpalmer@ou.edu
In final form 23 June 2022

AFFILIATIONS: Palmer, Bodine, Schvartzman, Kirstetter, and Zhang—Advanced Radar Research Center, and School of Meteorology, University of Oklahoma, Norman, Oklahoma; **Kollias**—Stony Brook University, State University of New York, Stony Brook, New York; **Zrnić**—NOAA/National Severe Storms Laboratory, Advanced Radar Research Center, and School of Meteorology, University of Oklahoma, Norman, Oklahoma; **Yu, Fulton, Salazar-Cerreño, and Yeary**—Advanced Radar Research Center, and School of Electrical and Computer Engineering, University of Oklahoma, Norman, Oklahoma; **Kumjian**—The Pennsylvania State University, University Park, Pennsylvania; **Cheong**—Advanced Radar Research Center, University of Oklahoma, Norman, Oklahoma; **Collis**—Argonne National Laboratory, Lemont, Illinois; **Frasier**—University of Massachusetts Amherst, Amherst, Massachusetts; **Hondl**—NOAA/National Severe Storms Laboratory, Norman, Oklahoma; **Kurdzo and Weber**—MIT Lincoln Laboratory, Lexington, Massachusetts; **Ushio**—Osaka University, Osaka, Japan; **Rowe**—University of Wisconsin–Madison, Madison, Wisconsin; **Torres**—Advanced Radar Research Center, and NOAA/National Severe Storms Laboratory, and School of Electrical and Computer Engineering, and Cooperative Institute for Severe and High-Impact Weather Research and Operations, University of Oklahoma, Norman, Oklahoma

Introduction: Science-driven radar-design principles

Technical decision process. Weather radars have improved our understanding of, and ability to forecast, increasingly frequent catastrophic weather events (Doviak and Zrnić 2006). These versatile instruments also have important applications to a broad range of other areas of atmospheric science, from gravity waves in the clear atmosphere to upper-atmospheric ice clouds in polar regions (Hocking et al. 2016). Radar design strategies depend on the atmospheric applications, requiring knowledge of the type of phenomena (e.g., rain, snow, cloud particles, turbulent eddies), its range, and its characteristic space and time scales. Scattering properties determine the attenuation and sensitivity constraints, which in turn set the radar wavelength, transmit power, and antenna parameters. Another important capability is dual polarization, which has become indispensable for microphysical studies of geometrically complex scatterers (e.g., oblate drops, hailstones, melting snow) and for quantitative estimation of precipitation amounts (Ryzhkov and Zrnić 2019; Oue et al. 2021; Bukovčić et al. 2020; Zhang et al. 2020; Matrosov et al. 2020; Ryzhkov et al. 2013a,b; Kumjian 2018).

Within the desired observation range, the spatial scales of interest determine the required range and angular resolution, which are controlled by the transmitted waveform bandwidth and antenna aperture. In addition, angular sampling in elevation (typically only 5–17 elevations for the WSR-88D) can be a limiting observational factor for mechanically steered antennas, which causes an undesirable trade-off in volume update time and the number of desired scans in elevation. This predicament is one reason for the interest from both the scientific and operational communities in phased array radars (PARs, see Fig. 1), which are steered electronically, providing finer angular sampling and beamsteering agility. This PAR capability provides vastly improved angular *sampling* but not angular *resolution*, with the latter being controlled by antenna aperture and radar wavelength for both dish and phased array antennas.

Another major scientific driver for radar design is the time scale associated with the phenomena of interest. Tornadoes, for example, evolve on the time scale of seconds (Bluestein et al. 2010, 2003; French et al. 2013; Houser et al. 2015), which requires an update time only achievable with an electronically scanned PAR, without impacting data quality or volumetric coverage or increasing limited transmission bandwidth. In addition, understanding the formation of severe hazards, such as hail and microbursts (Heinselman et al. 2008a; Newman and

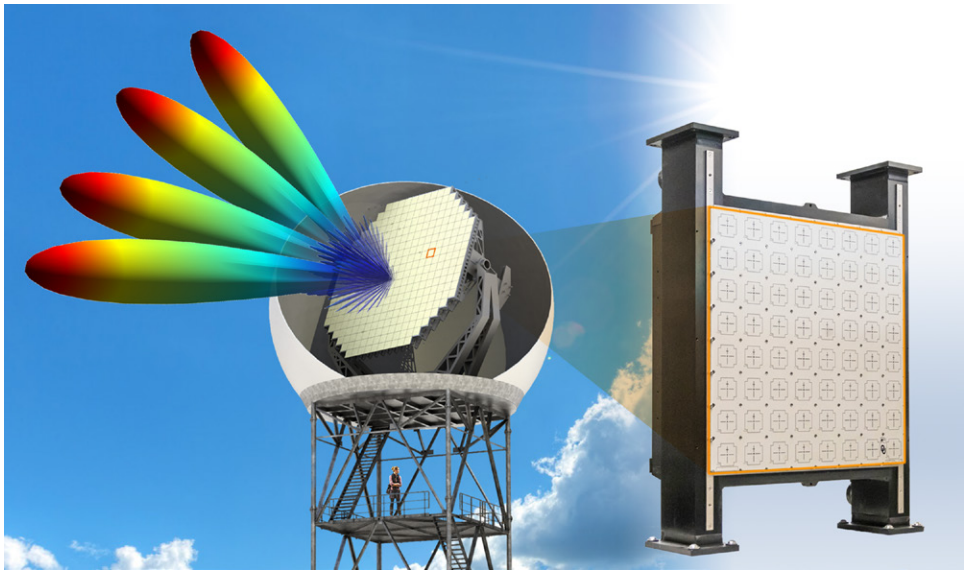

Fig. 1. An example phased array radar with a potential beam pattern and a closeup look of its radiating elements.

Heinselman 2012; Tanamachi and Heinselman 2016; Kuster et al. 2019), and capturing the evolution of deep convective updrafts requires rapidly collected volume scans through a deep vertical column (Emersic et al. 2011; Yoshida et al. 2017; Oue et al. 2018; Dahl et al. 2019; Kuster et al. 2019). In a PAR operational testbed, forecasters have noted substantial benefits of using higher temporal resolution data, including improved statistical performance of severe weather warnings issued (Heinselman et al. 2012, 2015; Bowden et al. 2015a; Bowden and Heinselman 2016; Wilson et al. 2017). Acceptable temporal resolution must be coupled with adequate spatial resolution to mitigate spatial smearing of rapidly evolving features.

The radar platform is another important consideration (e.g., fixed, transportable, mobile; ground-based, airborne, spaceborne). In many ways, radars on different platforms are complementary, but have their own unique advantages. Ground-based systems, especially mobile and transportable, can be deployed close to the phenomena, providing excellent angular resolution and sensitivity. They also offer the opportunity to observe the entire life cycle of storms because they are stationary during relatively long observation periods. Airborne systems have the advantage of being deployable where there is a lack of radar coverage (e.g., over the open ocean) but are inherently limited in focused observation time (temporal resolution) because the platform is moving (Hildebrand et al. 1996; Vivekanandan et al. 2014). They can also be used for "close up" observations of storms in land areas remote from ground radars (or blocked by terrain). Satellite-based systems have similar limitations but can provide a global view. Any moving platform is limited in size, weight, and power (SWaP) by either the platform itself (e.g., aircraft, satellite) or the transportation system (e.g., trucks on public roads). These SWaP constraints also drive many of the engineering design decisions mentioned above. Here, we focus on ground-based PAR technology, although these considerations can be applied more broadly.

Although science has primarily driven the major technical decisions highlighted in this description, other factors are inevitably part of the process. These factors, such as availability and maturity of technology and initial and recurring costs, are represented in the history of atmospheric radar science.

Historical perspective of atmospheric radar science. Although the exact origin is unknown, the first weather observations with radar likely occurred just before World War II (Doviak and Zrnić 2006). To radar developers, rain was considered "weather clutter" that obscured

observation of the desired targets. Although initially considered a nuisance, the military realized that weather clutter could serve a useful purpose, even offer a tactical advantage by indicating the precipitation distribution over the battlefield. The capability to penetrate through the cloud and map the three-dimensional (3D) structure of precipitation drew the attention of weather services, and at the end of World War II, the first weather radar networks emerged (Whiton et al. 1998). These early radars enabled recognition of basic storm features and advection/propagation, attributes of significant operational value to this day.

The first civilian network of weather radar in the United States was deployed by the Weather Bureau, which is now the National Weather Service (NWS). The radars were modified military units, used a 10-cm (S-band) wavelength, and had the designation WSR-1, WSR-1A, WSR-3, and WSR-4. In parallel, the U.S. military had its own weather radars, with some being part of scientific investigations (Massachusetts Institute of Technology, Illinois State Water Survey, Air Force Cambridge Geophysical Laboratories; see Whiton et al. 1998). Of note was a recording of a "hook echo" made by the Illinois State Water Survey on 9 April 1953 (Stout and Huff 1953). The first radar built specifically for weather observation was the WSR-57 (57 indicates the year of procurement, 1957). The motivating scientific factors for this deployment were the proven observation of hook echoes and the utility to measure precipitation in hurricanes, for which the 10-cm wavelength ensured minimal sensitivity reduction by attenuation.

The largest benefit both operationally and for scientific studies using radar occurred after introduction of the WSR-57. Never before was it possible to remotely identify the potential for tornado formation, hail shafts, and measure amounts of precipitation (Austin and Geotis 1990). In the 1960s, Doppler technology was nascent at universities and government laboratories. Doppler capabilities proved crucial for precise mapping of severe weather dynamics. Features like mesocyclones, tornadoes, strong wind gusts, microbursts, and macrobursts became visible on weather radar displays. These successes of Doppler information and promise for better estimates of the amounts of precipitation (Hudlow et al. 1985) justified the NWS decision to deploy its "flagship" weather radars, the WSR-88D (also referred to as NEXRAD; see Crum and Alberty 1993). Significant contributions enabled by Doppler processing include mapping of the 3D wind fields in supercell storms from two or more simultaneous Doppler measurements (dual-Doppler; Brandes 1977), direct measurements of tornadic winds from Doppler spectra, relationship of turbulence intensity to the Doppler spectrum width, and mitigating effects of hail shafts in three-body scattering (Zrnić 1987), among many. Assimilation of Doppler and reflectivity information into numerical weather prediction (NWP) models advanced the prediction of convection and severe weather (Caya et al. 2005; Tong and Xue 2005). The success of the Doppler technology was such that the Federal Aviation Administration commissioned the deployment of 45 Terminal Doppler Weather Radars (TDWRs; Evans and Bernella 1994) at major U.S. airports in response to a number of fatal commercial aircraft accidents caused by weather events (e.g., wind shear, microbursts).

The addition of dual-polarization capabilities to weather radars caused the next major leap forward in scientific and operational benefits (Ryzhkov and Zrnić 2019). Arguably, dual polarization made a greater impact than those afforded by Doppler. Whereas Doppler excels in identifying relatively rare hazardous phenomena (tornadoes, mesocyclones, downbursts) dual polarization's operational use and science apply to a broader range of phenomena. It can extract information about water substance and precipitation type in convective storms, tropical cyclones, stratiform precipitation, and winter storms. Moreover, use of dual-polarization information for quantitative precipitation estimation (QPE) significantly mitigated issues plaguing measurements with single-polarization radars (Ryzhkov and Zrnić 2019). Further, although scattering of electromagnetic waves by hydrometeors was an integral part of the science behind single-polarization radars, the advent of dual polarization greatly expanded this research area (e.g., Bringi and Chandrasekar 2001; Zrnić and Ryzhkov 1999). In addition

to vastly improving liquid- and ice-phase QPE, dual polarization has made positive impacts on flash flood warnings/forecasts (e.g., Cunha et al. 2013), detection and sizing of hail (e.g., Ryzhkov et al. 2013a,b; Ortega et al. 2016; Kumjian et al. 2019), classification of radar pixels and separation of meteorological from nonmeteorological returns (e.g., Park et al. 2009), detection of tornado debris (e.g., Ryzhkov et al. 2005; Bodine et al. 2013; Kurdzo et al. 2015), differentiating between tornadic and nontornadic supercell (Loeffler et al. 2020), and winter precipitation transitions and icing (e.g., Tobin and Kumjian 2017), among many others [see Kumjian (2018) for a review]. Dual-polarization radar's prowess has enabled assimilation of microphysical information into NWP models (e.g., Jung et al. 2008, 2010; Carlin et al. 2017).

Mobile ground-based polarimetric radars at X- and C-band wavelengths (3 and 5 cm) have become indispensable for field experiments (Biggerstaff et al. 2005; Bluestein et al. 2010; Wurman et al. 2012; Pazmany et al. 2013; Kurdzo et al. 2017; Geerts et al. 2017; Kollias et al. 2020). Even shorter-wavelength radars, such as W and Ka band, have also been used quite successfully for a variety of scientific applications (Bluestein et al. 2014), including increasingly important topics like wildfires (Aydell and Clements 2021). Mobility enabled storm interceptions as opposed to the old paradigm whereby stationary observers were at the mercy of the storm's unpredictable behavior. In addition to increasing angular resolution and lowering the beam height by proximity to the desired events, the probability of capturing storm-specific features (tornadoes, severe storms, etc.) increased dramatically, as witnessed by several successful field campaigns (Wurman et al. 2012). Dual-polarization studies of QPE at S, C, and X bands indicate that the relation between rain rate and specific differential phase is almost linear (Doviak and Zrnić 2006). This characteristic was extremely important at X band, in particular, for overcoming the effects of partial attenuation (Matrosov et al. 2002), which was arguably the greatest impediment for pre-dual-polarization rain measurements. Consequently, tremendous enhancement of weather observations at short wavelengths followed so that adverse events and significant precipitation relatively close to the radar could be quantified. Moreover, researchers suggested deploying closely spaced X-band radars to replace or complement the coverage by longer wavelength systems. At close range in a dense network the effects of Earth curvature are negligible and the lateral resolution per unit area improves (McLaughlin et al. 2009). Ongoing research aims at determining conditions under which a dense network of X-band radar may be more effective for weather observations over large metropolitan areas compared to a long-range surveillance radar (Chandrasekar et al. 2013).

Although PAR technology was initially conceived in the early 1900s (see, e.g., Haupt and Rahmat-Samii 2015), tremendous advancement of the technology was motivated by the need for advanced air defense capabilities during World War II. Over the past few decades, this technology has greatly matured in the context of air surveillance and defense applications, making PAR technology more accessible to other applications. The first PAR specifically modified to observe weather was the S-band SPY-1 radar on a Navy destroyer in 1997 (Maese et al. 2001; Robinson 2002). Following these observations, NOAA's National Severe Storms Laboratory (NSSL), with several private-sector, government, and university partners, developed the National Weather Radar Testbed (NWRT)—a SPY-1 antenna specifically modified to demonstrate the advantages of this new technology (Zrnić et al. 2007) for a next-generation operational radar network. The flat-panel antenna consisted of a slotted waveguide and vertically polarized radiators and was mounted on a rotating platform with a modified NEXRAD transmitter. Around this same time, other single-polarization PAR systems were developed, some on mobile platforms, allowing capture of a variety of weather events with unprecedented temporal resolution (Bluestein et al. 2010; Isom et al. 2013; Yoshikawa et al. 2013).

Combining dual polarization with the immense benefit of PAR beam steering is a challenge. Among one of the first mitigation strategies was Salazar et al. (2010) as part of the NSF

Collaborative Adaptive Sensing of the Atmosphere (CASA) program, where electronic beam scanning was employed in only the azimuth direction with mechanical steering in elevation. By doing so, the two transmitted polarizations were always orthogonal but not necessarily aligned with the Earth's surface since, as the array is tilted in elevation, the "horizontal" axis becomes nonparallel with the Earth's surface. This idea/challenge is explained in more depth throughout the paper. The next generation of X-band design with two-dimensional PAR steering has been developed by Raytheon for the CASA program and other applications (Puzella and Alm 2008; Frasier et al. 2018; Kollias et al. 2018).

Planar PAR antennas with electronic scanning only in elevation (mechanical in azimuth) avoid the orthogonality issue as well as tilting of the intended horizontal polarization. Such strategies have seen widespread implementation in China (Wu et al. 2018), an updated imaging radar by Toshiba Corp. (Kikuchi et al. 2020), and the Polarimetric Atmospheric Imaging Radar (PAIR) nearing completion at the University of Oklahoma's (OU) Advanced Radar Research Center (ARRC) (Yu et al. 2019). NSSL's Advanced Technology Demonstrator (ATD) (Stailey and Hondl 2016; Ivić et al. 2022) is a planar PAR capable of two-dimensional scanning, which requires polarimetric calibration per beamsteering position (Ivić et al. 2019). A unique cylindrical polarimetric phased array radar (CPPAR) was developed at the ARRC (Zhang et al. 2011; Fulton et al. 2017) based on theoretical studies that showed the effectiveness of such designs for maintaining polarization orthogonality, needed for polarimetric PAR observations.

The most advanced PAR architecture is a fully digital design, which holds promise for overcoming the challenge of combining polarimetric and PAR technologies (Fulton et al. 2016). Via element-level control, robust polarimetric calibration is possible, thus having the highest likelihood of attaining accurate rapid-scanning polarimetric observations for long periods without the need for recalibration. The all-digital "Horus" radar is currently under development at the ARRC with completion in 2022 (Palmer et al. 2019). This radar will be the first of its kind all-digital, polarimetric weather PAR with plans for exploiting its inherent scalability for applications requiring a large aperture.

The potential of phased array technology. Because of the confluence of previous development projects, technological readiness and reasonable cost, scientific need, and opportunity created by the eventual replacement of the WSR-88D network, now is the time to strongly consider PARs for atmospheric remote sensing. Compelling scientific discovery, as outlined in the companion paper by Kollias et al. (2022), will be enabled by the enhanced capabilities such as near-continuous-sampled range–height indicator (RHI) observations, unprecedented temporal resolution, adaptive/flexible scanning, and the potential of high-quality 3D wind estimation using passive, bistatic receivers along with PAR (Byrd et al. 2020, 2021). With all-digital PAR technology, which will be discussed later, the radar can become "software defined," allowing future observational modes to be implemented via software updates rather than expensive and time-consuming hardware changes. This all-digital architecture essentially creates a "future proof" radar extending the lifetime of such systems significantly. While convergence between the engineering and meteorological communities is a prerequisite, often collaborations are hampered by something as simple as a terminology gap between the communities. With the current interest and tremendous potential for scientific advancements, the community is in need of a concise and approachable tutorial on the technology, which is the purpose of this paper. The companion paper by Kollias et al. (2022) provides a more in-depth discussion on the scientific applications of this exciting technology.

Phased array radar fundamentals

Unique and flexible capabilities offered by PAR technology make this technology an attractive candidate for the next generation of weather radars (Zrnić et al. 2007). Key PAR capabilities

that support the needs of advanced weather surveillance include the ability to almost instantly steer the radar beam to an arbitrary direction within the scan sector (i.e., *beam agility*), the ability to digitally form multiple simultaneous beams in different directions, and the flexibility to dynamically redefine the sampling parameters for each beam position in the scan. In this section, we introduce these capabilities and discuss how they are critical for advancing atmospheric science.

How does a PAR work? PAR is based on the concept of an interference pattern. Assume we have a tank filled with water; now, two rocks are held at the same height above the water level, separated by a distance d. Then, the rocks are dropped in the water at the same time, and propagating wave patterns start forming out of the points in which the rocks entered the water. These locations will be referred to as the wave phase centers, where the propagation starts. The waves propagate along the surface, forming concentric circles around the phase centers (Fig. 2a). Notice that the circles intersect in certain directions where the crests of waves from the two different sources collide. According to superposition, the effect caused by two or more independent perturbations is the sum of the individual effects that would have been caused by each perturbation individually. Applying this concept, we can observe that the directions on which the wave crests collide produce *constructive interference*. In this case, each individual wave is at its crests and the wave resulting from their interaction has a crest that is double the height of the individual ones (see Fig. 2b). In contrast, there are directions where the propagating wavefronts are such that the waves interact producing *destructive interference*. In this case, the crest of one wave is summed with the valley of the other one, and through superposition they cancel. In summary, when we have two sources of waves propagating in the same plane, there are certain directions where the energy is summed constructively and others where it is summed destructively.

A PAR is an arrangement of antenna elements transmitting/receiving independent electromagnetic waves into/from free space. It can create patterns of constructive interference in specific directions, similar to those in the water tank example. The number of phase centers or antenna elements N is typically much larger than two. An illustration of a uniform linear array is presented in Fig. 3a, where the direction determined by the normal to the array plane is referred to as *broadside*. Antenna elements are separated by $d = \lambda/2$, where λ is the radar

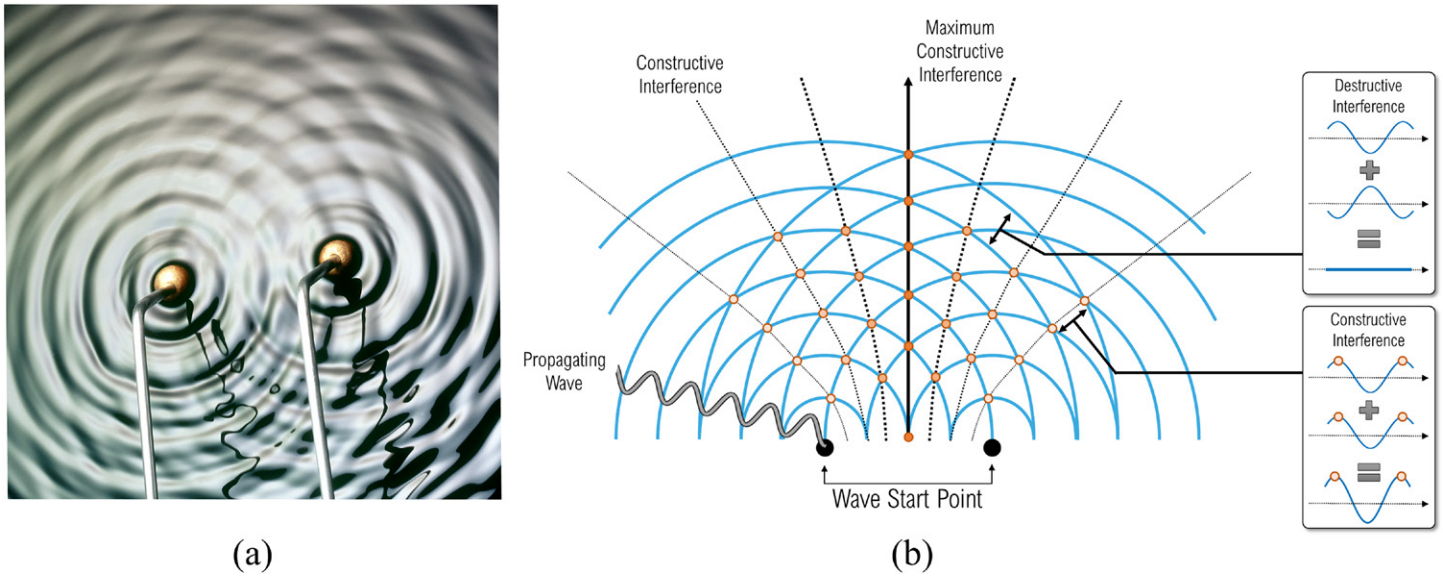

Fig. 2. Wave interference pattern: (a) two-wave ripple tank and (b) depiction of the propagating waves forming patterns of constructive and destructive interference. Image in (a) used with permission from Fundamental Photographs (www.fphoto.com).

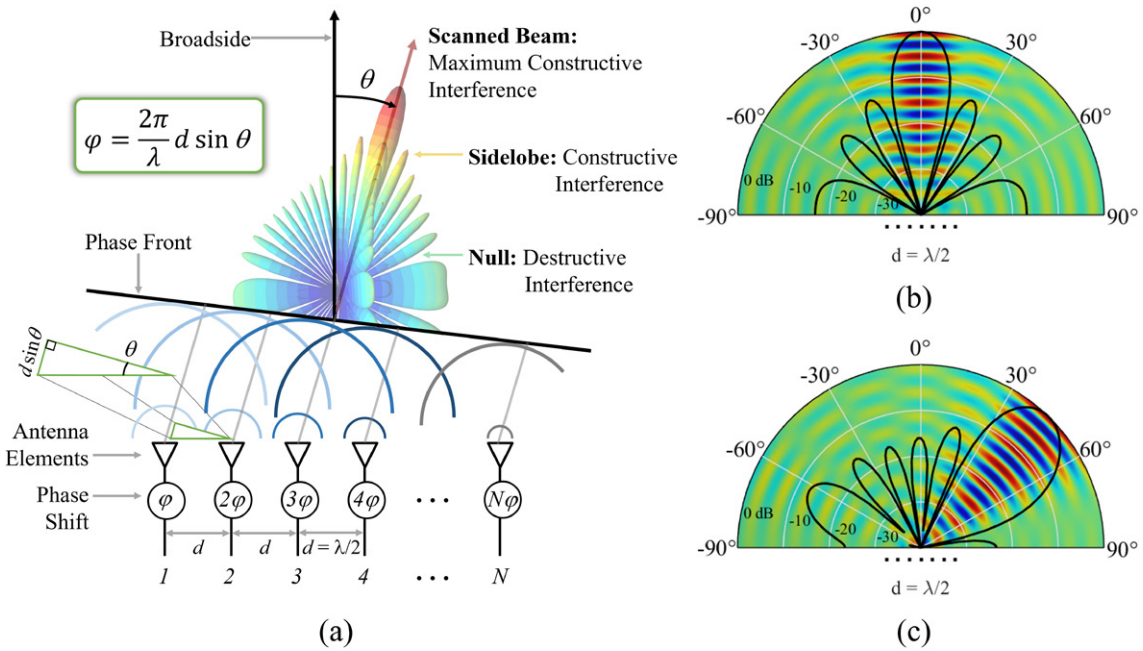

Fig. 3. Fundamental concepts of a PAR (a) uniform linear array. The illustrative PAR is composed of *N* antenna elements spaced by $d = \lambda/2$ with phase shifters offset by ϕ in the sequence from left to right. That produces a beam steered to the θ angle which sets the direction of the scanned beam. Note that $\theta = (2\pi / \lambda) d \sin\theta$, due to the time delay needed for wavefronts to align in the scanned beam direction, as shown in the triangle between the first two elements. Color shading represents the relative gain, where blue tones represent lower values and red tones represent higher values. (b) Azimuthal dependence of the antenna radiation pattern at broadside. (c) Azimuthal dependence of the antenna radiation pattern steered to +45°. For (b) and (c), color shadings illustrate the peaks and crests of the propagating waves (as in Fig. 2), with higher values indicating regions of constructive interference and near-zero values (in tones of green) indicating regions of destructive interference.

wavelength in free space, to mitigate *grating lobes* (i.e., many directions with maximum constructive interference; Delos et al. 2020). As in the previous case, when the antenna elements are excited with sinusoidal signals, the array creates an interference pattern with certain directions with constructive and destructive interference. Close to the antenna elements the beam is formed in the so-called reactive near field. Emerging from this region the wave propagates through the radiative near field (also called the Fresnel region). As the distance from the antenna increases, wave fronts become nearly planar and the wave propagates in the far field (also called the Fraunhoffer region). The angular distribution of radiated power in the far field is defined as the antenna radiation pattern, and it is used to characterize the electromagnetic radiation properties of the antenna. Note that dish-antenna radars are also characterized by their antenna radiation pattern, one of the key differences with PAR being the electronic steering capability. The direction of maximum constructive interference is defined as the *mainlobe* and determines the scanning beam position. Other directions with partially constructive interference determine the location of the *sidelobes*. These are undesirable because they can contaminate the expected measurements being observed through the mainlobe illumination. Note that all practical antennas (including those on the WSR-88D) have a mainlobe and sidelobes surrounding the mainlobe.

The mainlobe of a PAR can be electronically *steered* to different angles by varying the difference in phases between adjacent antenna elements. The phase of a signal (ϕ) is proportional to its propagation time ($\phi = 2\pi ft$, where f is the radar frequency and t is the time), so we can think of a phase difference as an equivalent time delay. Specifically, to steer the beam to a direction θ with respect to the array broadside (i.e., direction perpendicular to the plane of

the antenna), the *phase fronts* from all elements have to align to create maximum constructive interference. Notice that this can be accomplished by introducing a constant phase difference of φ (or, equivalently, a time delay) between adjacent elements. As shown between the first two antenna elements of Fig. 3a, to create this constructive interference the spatial distance between crests of signals in adjacent elements has to be $d\,2\sin\theta$. This distance can be expressed in terms of phase using the wavenumber, $k = 2\pi/\lambda$. Thus, to steer the PAR beam to point at an angle θ with respect to the broadside, the phase difference between adjacent elements has to be set to $\varphi = kd\,2\sin\theta$. Finally, Figs. 3b and 3c present azimuth cuts of the two-dimensional radiation patterns, to compare a beam at broadside with one steered to $\theta = 45°$. Notice that as the beam is steered off the broadside, the width of the mainlobe increases, which translates directly to a change in angular resolution. This increase in mainlobe width is due to the smaller apparent antenna aperture scanning an angle off broadside. That is, when scanning at broadside the full aperture is used, however, only the projection of the aperture on a plane orthogonal to the steering direction is used when scanning off broadside Skoinik (2008).

Advanced PAR scanning concepts and associated potential artifacts in meteorological data have been an important subject of study in recent publications by Schvartzman and Curtis (2019), Torres and Schvartzman (2020), Nai et al. (2020), Schvartzman (2020), Schvartzman et al. (2021b), and Boettcher et al. (2022). For instance, the electronic steering of the beam off the broadside introduces beamsteering biases (due to co- and cross-polar antenna patterns) in reflectivity and polarimetric variables. Another example involves the use of radar imaging, which increases two-way sidelobe levels considerably, and thus, can introduce large biases in reflectivity when used to scan a high gradient. Ideally, no PAR-induced artifacts should be seen in meteorological data, as the scanning techniques should be selected carefully to mitigate these. Selecting the appropriate scanning mode involves adaptive scanning (discussed later in this section), whereby radar-induced artifacts would be mitigated.

PAR capabilities.

Beam agility. Beam agility is the capability of steering the radar beam to different angles within the scan sector almost instantly (on the order of microseconds) without mechanically rotating the antenna. It is only possible with phased array antennas and is one of the key advantages of stationary PARs over rotating dish-antenna systems. The agile beam capability enables PARs to quickly switch the scan sector to observe different regions of interest. Whereas it may be possible to operate a rotating dish system to scan only certain regions with meteorological targets of interest (Kuster et al. 2019), this would take longer than an agile-beam PAR to scan the same regions, with the same acquisition parameters. Additionally, this mode of operating dish-antenna-based systems introduces significant wear in the mechanical parts and is not conventionally used in operations.

Several applications that exercise the agile beam steering capability of PARs have been proposed for weather observations (Heinselman et al. 2013; Torres et al. 2016). For instance, Yu et al. (2007) demonstrate the use of *beam multiplexing*, whereby the PAR's beam agility is exploited to increase the number of independent samples by rapidly pointing to widely separated angular positions. The main advantage of this technique is that it allows a reduction on the number of samples (hence scan time) to achieve the same standard deviation of estimates. The main disadvantage is that because samples are not collected in a continuous *coherent* sequence, spectral processing methods cannot be used (e.g., ground clutter filtering). This PAR system's multichannel receiver helped make these algorithms possible (Yeary et al. 2012). Another PAR technique that exploits beam agility is called motion-compensated steering Schvartzman et al. (2021a). It exploits electronic steering to improve azimuthal resolution of polarimetric Rotating PAR (RPAR). Furthermore, we note that beam agility can greatly increase the effectiveness of adaptive scanning techniques, by which the scanning

strategy is dynamically evolving to improve observations of meteorological echoes of interest. While most techniques mentioned here are independent, they could be used simultaneously provided there is no impact on data quality.

Imaging. Radar imaging involves transmitting a wide antenna radiation pattern to illuminate a large sector and using digital beamforming (DBF) to simultaneously form multiple receive beams within the illuminated sector. DBF radar beams are formed by means of digitally combining signals received from subarrays or antenna elements with digital outputs. The principle is that backscattered energy is received from the wide sector illuminated by the transmit beam and signals are digitally sampled at different spatial locations in the PAR antenna plane. These digital in-phase and quadrature (IQ) samples are taken simultaneously, and by means of digitally steering a pencil receive beam (i.e., in software), we can create constructive interference in desired directions. The concept of DBF was initially proposed by Barton (1980) and Steyskal (1988) and has been widely used to develop advanced scanning and signal processing techniques for applications including wireless communications (Chryssomallis 2000; Sadhu et al. 2017; Roh et al. 2014), air surveillance and defense (Van Veen and Buckley 1988; Brookner 2002; Talisa et al. 2016), biomedical (Peterson et al. 1987), oceanography (McIntosh et al. 1995), atmospheric boundary layer (Mead et al. 1998), and weather radar observations (Isom et al. 2013; Yoshikawa et al. 2013; Curtis et al. 2016; Nai et al. 2016; Kikuchi et al. 2017; Mizutani et al. 2018; Kurdzo et al. 2017; Schvartzman et al. 2021c).

The "spoiled" transmit beams (i.e., wider beamwidth) are commonly synthesized by varying the magnitude and phase of transmit signals at each individual array element (commonly referred to as *tapering*) in an active PAR (see Fig. 4). Other types of antennas can be used to transmit wide beams, as demonstrated by Isom et al. (2013) with the Atmospheric Imaging Radar (AIR), where a slotted waveguide passive array is used to transmit a fixed "fan" beam. The wider transmit beam comes at the expense of increased two-way antenna sidelobe levels, reduced two-way antenna gain (i.e., reduced ability of the antenna to radiate in a specific direction), and slightly increased beamwidth. The reason for the increase in sidelobe levels (also in beamwidth) is that the two-way beam is the mathematical product of the one-way beams (in linear units), and since the spoiled transmit beam has high gain where the receive beams have sidelobes, their levels are not reduced. In contrast, when using pencil beams on transmission and reception, one-way sidelobe levels are squared and farther reduced. The C-band mobile PAIR being developed by the

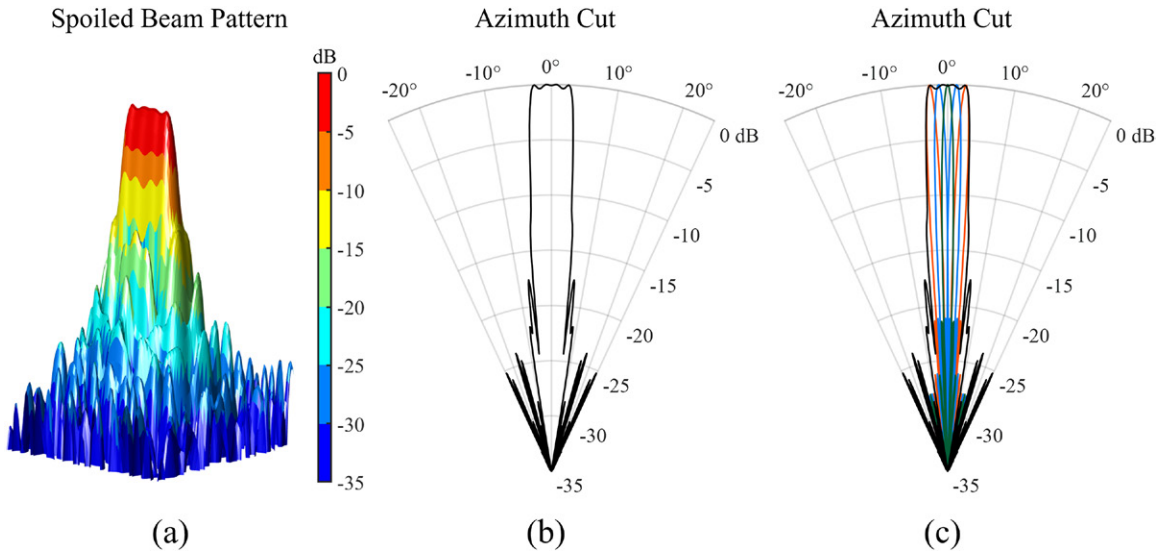

Fig. 4. Illustration of radar imaging, whereby a wide transmit beam can illuminate a large sector and simultaneous receive beams are formed within transmit beam. (a) Spoiled transmit beam. (b) Azimuth cut of the transmit beam. (c) Azimuth cut of beams received by digital beamforming.

ARRC is the evolution of the AIR system and includes dual-polarization capabilities with radar imaging (Salazar et al. 2019; Yu et al. 2019; Schvartzman et al. 2022).

The concept of DBF was proposed decades ago for PAR systems and has been recently demonstrated for both single- and dual-polarization weather observations using stationary PAR and RPAR systems (Isom et al. 2013; Kurdzo et al. 2017; Kikuchi et al. 2020; Schvartzman et al. 2021c). Nevertheless, DBF creates new advanced scanning concepts that should be investigated for the different PAR architectures. That is, through beam pattern synthesis methods (Mailloux 2017; Hansen 2009), transmit beams could be spoiled in either azimuth only, elevation only, or both azimuth and elevation. While not all of these concepts have been considered for weather observations, they may provide ways to reduce the scan update times by trading other radar resources (e.g., sensitivity, angular resolution), hence providing drastically improved temporal resolution to capture storm dynamics. Pattern synthesis can enhance atmospheric remote sensing by using beams with different characteristics to scan precipitation systems and minimize loss in spatial resolution and/or sensitivity. For example, spoiled beams may be convenient for weather with relatively smooth reflectivity gradients (due to higher sidelobe levels), while a synthesized beam with three separate mainlobes may be better for convective storms with sharp reflectivity gradients Torres and Schvartzman (2020). Furthermore, practical imperfections from antenna manufacturing can be corrected using beam synthesis, to match the far-field H/V synthesized patterns and mitigate copolar antenna biases Schvartzman et al. (2022). In summary, this capability is not feasible with rotating-dish systems but can be considered mature for the polarimetric PARs.

Adaptive scanning. *Adaptive scanning* refers to a radar's ability to rapidly change scanning strategy (e.g., combining beamforming and agile beam steering) to focus radar resources on constantly evolving meteorological echoes of interest. Adaptive scanning algorithms are capable of managing radar resources to selectively improve the temporal resolution, spatial sampling and/or data quality of meteorological observations. These algorithms aim to maximize the use of these resources and provide users critical information in a timely manner (Torres and Schvartzman 2020). For instance, severe storms can develop in minutes (Heinselman et al. 2008b), presenting a challenge to forecasters if update times are relatively slow. In fact, current experiments strongly suggest that radar data with high temporal resolution could increase warning lead times of hazardous weather events (Heinselman et al. 2012; Bowden et al. 2015b). Adaptive scanning provides faster update times supporting development of conceptual models of fast-evolving convective storms.

Adaptive scanning has been implemented on dish-antenna radars and PARs. Chrisman (2009) developed the Automated Volume Scan Evaluation and Termination (AVSET) technique which dynamically controls the number of scanning angles in elevation based on the observed meteorological returns. AVSET terminates the current volume scan if minimum thresholds for reflectivity are not met, shortening the volume scan time. This technique has been operational on the WSR-88D network since the early 2010s. McLaughlin et al. (2009) demonstrated adaptive storm sampling capabilities with a small network of X-band dish-antenna systems as part of the NSF CASA project. However, the effectiveness of adaptive scanning techniques is limited for dish-antenna radars owing to the mechanical inertia of the rotating antenna and the lack of beam agility and/or beamforming capabilities.

Adaptive scanning techniques are most effective with the PAR technology. Torres et al. (2016) demonstrated the Adaptive Digital Signal Processing Algorithm for PAR Timely Scans (ADAPTS) technique with the single-polarization NWRT by identifying beam positions with significant meteorological returns in real time and scheduling the beams to scan these with the goal to reduce the scan time. Schvartzman et al. (2017) proposed an adaptive scanning algorithm, based on a model of the human attention system, capable of defining sectors

of meteorological interest to be scanned by the radar. Figure 5 illustrates three adaptive scanning concepts proposed by Torres and Schvartzman (2020), namely, a significance-based selection of sectors to scan (e.g., the sector in black is deemed nonsignificant and therefore not scanned), a dynamic determination of the pulse repetition times (T_s in the figure are different PRTs) based on the range/velocity of storms, and a spatial resolution driven imaging beam selection technique where different spoiled beam factors are a function of storm structure.

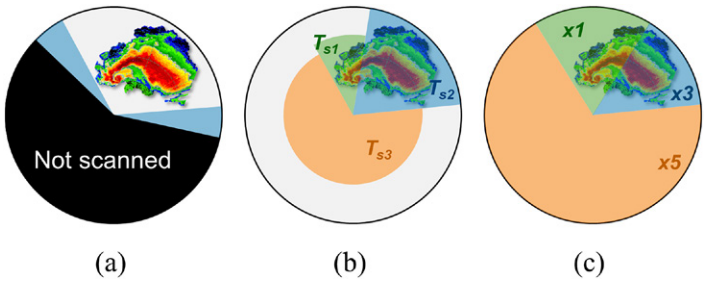

Fig. 5. Adaptive scanning concepts: (a) a significance-based selection of sectors to scan where the sector in black is deemed nonsignificant and therefore not scanned; (b) a dynamic determination of the pulse repetition times, where the T_s in the figure are different PRTs based on the range/velocity of storms; and (c) a spatial-resolution-driven imaging beam selection where different spoiled beam factors are used as a function of storm structure, where *x*1 is a pencil beam and *x*3 and *x*5 are beams spoiled by factors of 3 and 5.

PAR architectures. PARs can be designed according to different architectural principles, driven by the application and functional requirements. The PAR architecture determines which capabilities (e.g., radar imaging) are feasible with the system. Architectures for atmospheric applications can be classified into four groups: analog beamformer, fixed imaging, subarray beamformer, and all-digital beamformer, which are presented in Fig. 6 and described in the following sections. Fixed imaging is an inexpensive way of implementing radar imaging (as done in the AIR system) and can be considered as a particular case within the subarray beamformer category. Therefore, it will not be explicitly described hereafter. We note that the antenna geometry (four planar faces, cylindrical, etc.) and the element arrangement

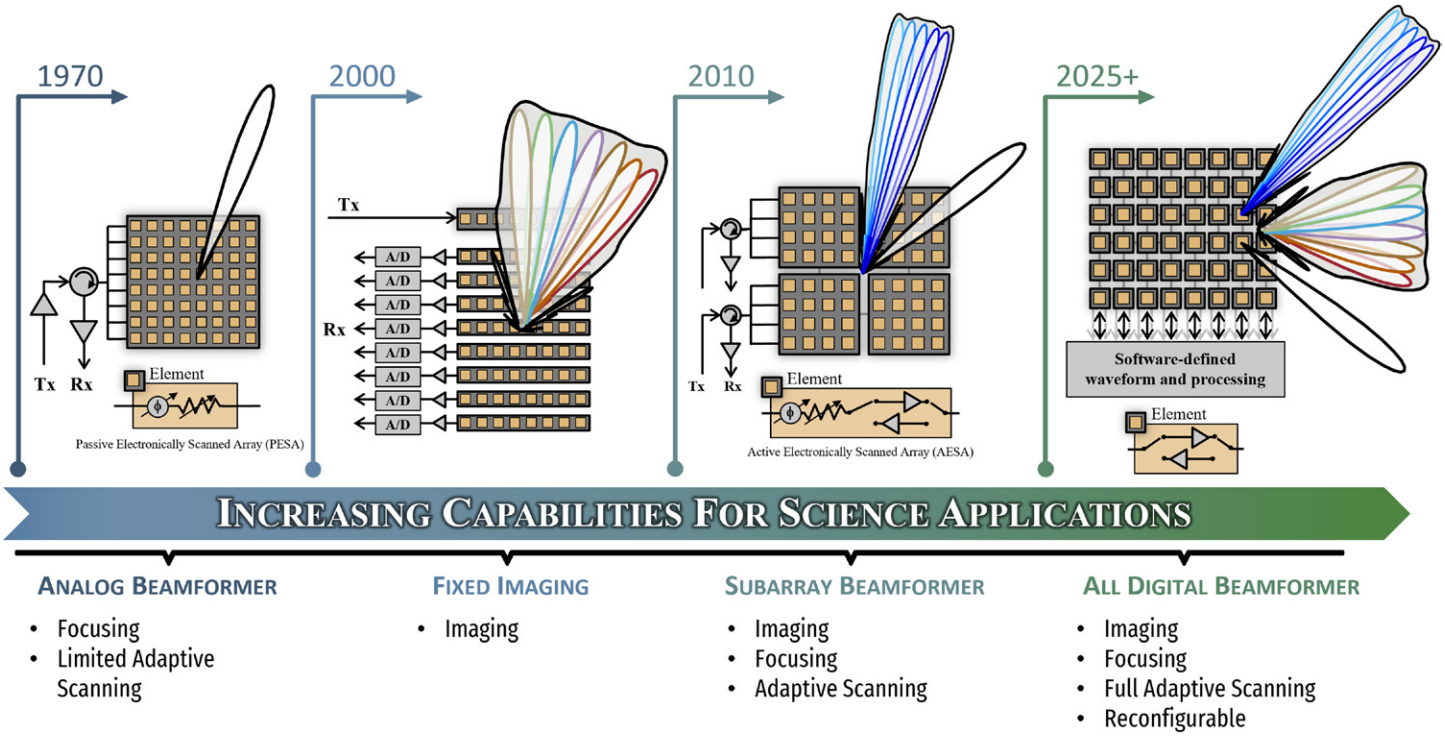

Fig. 6. PAR architectures designed for atmospheric applications: analog beamformer, fixed imaging, subarray beamformer, and all-digital beamformer.

(e.g., square or circular, uniform, or triangular lattice) may also be considered part of the PAR architecture, but we focus on the single-face planar PAR in this article. Further, note that these architectures can be used in a concept of operations where the phased array antenna may be stationary or rotating (Schvartzman 2020).

Analog beamforming. Analog beamforming systems form transmit and receive beams through an analog beamforming network and can have either distributed transmit/receive (T/R) modules across elements (active) or a single high-power transmitter (passive). PARs based on an analog beamforming network can steer electronically but cannot use imaging or DBF. Through electronic steering and the ability to change scan parameters (e.g., PRT, number of samples per radial), these systems are capable of rudimentary adaptive scanning. A limitation of the passive version of this architecture is that the transmitter is a single point of failure.

The SPY-1A PAR installed at the NWRT was based on a passive analog beamformer architecture. A single high-power amplifier provided 750 kW to the array on transmission, and a single digital receiver produced IQ samples used to estimate radar variables. This PAR system was fundamental for demonstrating capabilities of PAR technology for weather observations, like rapid scanning (~1-min volume scans; Heinselman et al. 2013) and beam multiplexing (Yu et al. 2007) through agile beam steering and adaptive scanning (Torres et al. 2016).

Sub-array digital beamforming. Systems that can sample the received fields and produce digital signal outputs for sub-arrays of antenna elements have more capabilities than analog beamformers. In sub-array beamforming PARs, the output signals from groups of antenna elements are summed to produce a *sub-array beam*. The signals received by the sub-arrays are transformed appropriately (e.g., down converted in frequency) and sampled with analog-to-digital converters. Then, groups of digital signals produced by the sub-arrays can be simultaneously combined (digitally) in multiple ways to produce different beams. That is, the use of digital beamforming enables the application of desired phase offsets on received signals (similar to the concept presented in Fig. 3), such that maximum constructive interference is formed in certain directions to produce beams. There are two main limitations of this architecture. First, digital beams can only be formed within the antenna pattern of the sub-array, which limits the field of view for imaging. Second, the use of sub-arrays creates grating lobes in their antenna patterns, because their phase centers are separated by distances greater than half-λ (Mailloux 2017; Hansen 2009). This limits the degrees of freedom to control sidelobe levels in the two-way PAR antenna pattern.

The ATD and the PAIR radar systems are based on sub-arrayed architectures. The ATD radar has 4×2 panel-based sub-arrays in rows and columns, for a total of 512 antenna elements per sub-array. These sub-arrays are overlapped (i.e., elements can be part of a few different sub-arrays) to minimize the influence of grating lobes in the overall antenna pattern. This gives the ATD radar flexibility to exploit DBF within the sub-array pattern mainlobe, ~12° in the horizontal plane and ~4° in the vertical plane to scan multiple beams simultaneously. The PAIR radar has nonoverlapped sub-arrays grouping two rows of elements through the whole array. This gives the PAIR system high flexibility in using DBF along the vertical plane, within its sub-array pattern (~45°), to scan multiple elevation angles simultaneously.

All-digital beamforming. Systems that produce digital signal outputs at each antenna element are referred to as all-digital radars (Fulton et al. 2016). The all-digital architecture gives the highest flexibility to exploit PAR capabilities like beam agility, DBF, and adaptive scanning. These radars can scan narrow pencil beams or wide imaging beams in any direction (azimuth/elevation) without the limitations of a sub-array architecture. Having digital signals at every element makes this architecture a *software-defined* radar, because the array can be

reconfigured via software. This architecture can also be considered *future proof* as it already implements the maximum level of digitization possible with a PAR and gives the highest degrees of freedom for future experimental needs involving dynamic array reconfiguration. Furthermore, all-digital systems may enable new polarimetric calibration modes based on measuring the mutual coupling (essentially cross talk among elements) of individual antenna elements (Lebrón et al. 2020). In summary, the main advantages of an all-digital beamformer include the ability to use a wide variety of synthesized beam patterns and scanning strategies, to automatically recalibrate the array on the fly using mutual-coupling measurements, to exercise space–time processing of signals for better clutter mitigation, to largely mitigate cross-polar pattern contamination, and to produce high-accuracy measurements free from grating lobes. Disadvantages include high data rates and high real-time control/processing software complexity. However, with the continuous and rapid advancement of modern electronic devices, data rates and software complexity are becoming a more tractable challenge.

The Horus all-digital radar being developed by the ARRC is a polarimetric S-band system with this architecture (Palmer et al. 2019; Yeary et al. 2021). Horus is expected to be operational in 2022 and will be the first-ever polarimetric all-digital radar for weather observations. This proof-of-concept system will be used to demonstrate the benefits of all-digital technology for atmospheric observations, although considering its relatively wide beamwidth (~4°), it may not produce high spatial resolution measurements of precipitating systems. Leveraging the scalable architecture of the Horus radar, full-scale systems with a 1° beamwidth at broadside have been conceived (Palmer et al. 2022). The capabilities of such systems would enable transformative scientific discoveries in the atmospheric sciences, with unprecedented spatial and temporal resolution.

Summary of PAR advantages. Ongoing research efforts aimed at demonstrating the advantages of PAR technology for atmospheric observations indicate that PARs will enable revolutionary scientific breakthroughs. The flexibility to electronically steer the radar beam and scan different regions of the atmosphere almost instantly enables rapid volumetric scanning of storms. This feature, coupled with the ability to change the shape of the radar beam via imaging and the scanning parameters using adaptive scanning, places the PAR technology in an unparalleled position for scanning unpredictable and rapidly evolving hazardous weather. PARs with high spatial and temporal resolution can enhance the quality of observations by utilizing advanced clutter and interference mitigation techniques (Curtis et al. 2016; Lake et al. 2016). Higher levels of digitization are desirable in general, with an all-digital system providing maximum flexibility for future needs.

Challenges and areas of needed research

Although significant research has been accomplished, as with any emerging technology, challenges with PAR for atmospheric applications do exist. This section summarizes the primary technical challenges and proposes possible avenues to solutions.

Calibration-varying beam and polarization characteristics.

Beam characteristics. With a goal of quantitative observations of the atmosphere, it is crucial and challenging to fully characterize the PAR beam properties and to accurately calibrate PAR weather observations. The challenges come because the beam characteristics of a typical planar PAR change as a function of electronic beamsteering, unlike a dish antenna radar that has a fixed beam. The changing beam with pointing direction is typically not an issue in hard-target detection for military radar, but is a significant drawback for quantitative weather measurements. Typically, polarimetric weather radar measurements require a high accuracy of 1 dB for reflectivity (Z_H), 0.2 dB for differential reflectivity (Z_{DR}), 0.01 for copolar

correlation coefficient (ρ_{hv}), and 3° for differential phase (ϕ_{DP}) (NOAA 2015). Unfortunately, the bias/error caused by the varying PAR beam characteristics can be much larger than the required accuracy. For example, the two-way scanning loss due to the projected beam aperture reduction (beam broadening) and anisotropic element pattern can cause up to 6 dB difference in reflectivity measurement if a PAR points to 45° away from its broadside direction. When the effects of mutual coupling (e.g., essentially cross talk among elements) are taken into account, the PAR beam must be formed through an optimization process with full characterization and calibration. The mutual coupling causes the active element patterns to be irregular, from which the overall best full array beam pattern cannot be formed with analytical approaches. The optimization process uses the active element patterns with mutual coupling taken into account and adjusts the weights for each element to achieve the best array beam pattern that meets objectively defined goals. Calibration can be accomplished by finding the correct radar constant through quantifying the direction-dependent beamwidth and antenna gain by analysis and/or measurement. Additionally, amplitude and phase calibration of each element is critical for achieving low sidelobes (e.g., Fulton et al. 2016).

Polarization inequity and cross coupling. In addition to accurate measurement of reflectivity factor, polarimetric radars must ensure that the dual-polarized (H and V) fields are perpendicular with the H-polarization aligned with the Earth's surface. For dish-based radars, this polarimetric calibration task need only be completed for a single bore-sight beam with the dual-polarized fields orthogonal to each other, like latitude and longitude directions on the globe. The polarimetric calibration challenge is arguably the most daunting, with potentially thousands of beam positions. As shown in Fig. 7, the electric fields produced by the H and V radiating elements are in general nonorthogonal, with the degree of nonorthogonality a function of beam direction (Zhang et al. 2009). The two sets of lines shown in red and blue in Fig. 7 represent H and V fields. Note that the spherical surface represents the coordinate system of the PAR antenna as it takes measurements at different steering angles. The mapping from this coordinate system to the more traditional Earth-relative system (e.g., azimuth/elevation) consists of applying a set of trigonometric transformations (Ivić 2017; Schvartzman et al. 2021a). An interesting characteristic is that the H and V fields are coupled, except for beam in the principal planes (horizontal and vertical lines in the Fig. 7). PARs with different radiating elements (e.g., aperture, patch) exhibit similar imbalance and cross-coupling issues along the latitude lines as shown in Lei et al. (2013, 2015). These imbalances and cross-coupling issues are undesirable, causing

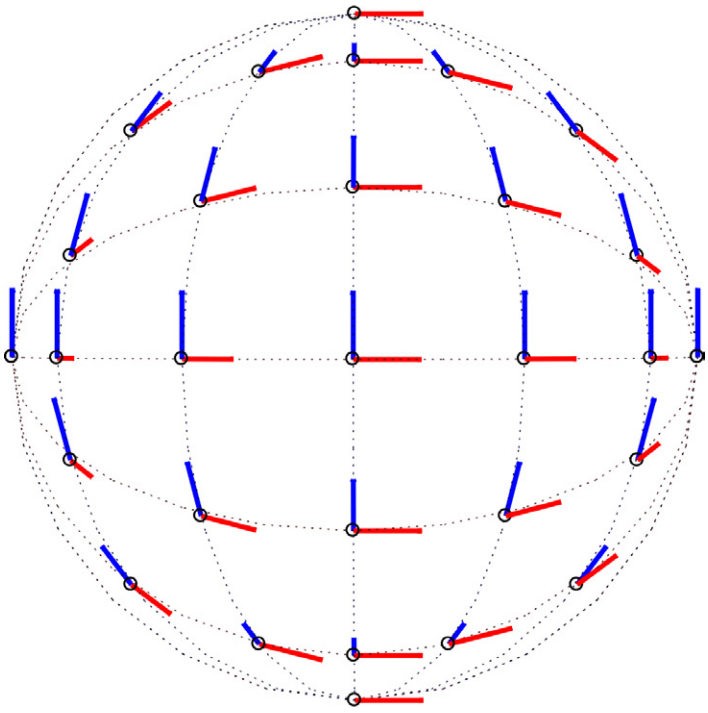

Fig. 7. Conceptual sketch of unbalanced and coupled electric fields on a spherical surface radiated from a pair of radiating antenna elements at the center. The red and blue lines represent the H and V electric fields. Note that the spherical surface represents the coordinate system of the PAR antenna as it takes measurements at different steering angles.

substantial bias in measurements of Z_{DR}, ρ_{hv}, and ϕ_{DP} that can be much larger than the tolerable errors and need to be calibrated/corrected.

Polarimetric calibration. PAR polarimetric calibration can be accomplished through careful theoretical analysis, system simulations, and calibration experiments (Zhang et al. 2009; Zrnić et al. 2011). In these approaches, polarimetric calibration can be performed on either time series IQ data or radar-variable data. In the case of time series data, the relation between the electric field at the hydrometeors and that at the radar antenna coordinate is established through a projection matrix, and a correction matrix is derived to convert the PAR measured scattering matrix to the intrinsic scattering matrix providing unbiased polarimetric radar estimates, as formulated by Zhang et al. (2009) for dipole antennas and by Lei et al. (2013) for aperture and patch antennas. When the PAR scattering matrix is measured using alternating transmission, the Doppler effects need to be taken into account as proposed by Zrnić et al. (2011) because scatterer motion causes a phase shift between pulses. The beam-dependent biases of the PAR measured/estimated polarimetric radar variables are calculated/measured for every beam direction, and then subtracted from the PAR estimates (Zhang et al. 2009; Lei et al. 2013). Using broadside-beam measurements from a PAR with mechanical scan capability or comparisons to a well-calibrated dish radar are methods for validating PAR polarimetric performance as shown by Ivić and Schvartzman (2019, 2020), Li et al. (2021), and Heberling and Frasier (2021). Both calibration methods can mitigate biases. The main advantage of using time series data is the flexibility to generate accurate radar variables directly (with calibrated IQ data). The main limitation is that it requires more computing power to apply the corrections at the IQ level in real time and may be more time consuming.

Although polarimetric calibration is a significant challenge for PAR, initial exploration using testbed PARs provides evidence that the necessary accuracy of variables can be achieved (Ivić 2019, 2021; Ivić et al. 2020; Weber et al. 2021). In particular, we note that calibration of Z_{DR} and ϕ_{DP} as a function of steering angle may be more challenging than that of ρ_{hv}. This is because ρ_{hv} is defined as the normalized cross correlation of copolar H/V beams, and since both are changing similarly as the beam is steered off broadside, biases in ρ_{hv} due to the PAR antenna patterns are negligible (assuming well-matched broadside beams). The latest results reported by Weber et al. (2021) indicate a calibration accuracy of ±0.25 dB for Z_{DR}, ±2.1° for Φ_{DP}, and ±0.01 for ρ_{hv} (see Fig. 15 in Weber et al. 2021). It is noted that the stability of the calibration coefficients (i.e., how often it needs to be recalibrated) depends on the particular system architecture and implementation, and it is a topic of current research.

Comments on cost. In the atmospheric science community, cost is often mentioned as a key obstacle to the widespread adoption of PAR technology (Herd and Conway 2016) and is certainly a complex topic requiring an in-depth analysis that cannot be provided in this primer. However, it can be said that although certainly more expensive than a traditional dish radar, the significant advantages of PAR technology outweigh the initial cost, especially when the software-defined nature of an all-digital architecture is taken into account. As emphasized before, an all-digital PAR can be reconfigured via software upgrades rather than costly hardware modifications, thus reducing the lifetime maintenance and operations costs. Any PARs developed for the scientific community will rely heavily on previous development work in both the defense sector and the rapid growth in the wireless communications industry. Furthermore, any nationwide operational network of PARs would represent the single largest weather radar procurement in U.S. history, which would justify development of custom application-specific integrated circuits (ASIC), replacing other power-hungry and costly electronics. It is emphasized that these ASICs would reduce the overall system cost and power requirements while retaining the reconfigurability and advanced capabilities of an all-digital PAR.

Vision for the future of observational atmospheric science

Phased array radars will broaden the range of scales observed from seconds to years, enabling synergistic studies with other observations of thermodynamic, dynamic, and microphysical processes to bridge across weather and climate studies. The scientific community has strong interest in collecting such observations to document fine-scale processes associated with high-impact weather events that are partly conditioned on climate change with the goal of improving weather forecasts and climate models.

Science-driven radar system design trade space. The atmospheric science community extensively uses different radar wavelengths that provide complementary capabilities for capturing different meteorological phenomena. For the sake of simplicity, we define "long wavelengths" as those in the S band (8–15 cm). Most precipitation particles are small compared to these wavelengths, and thus scattering can be accurately treated using the Rayleigh approximation. Further, because attenuation is minimal, radar coverage is maximized. As such, S-band wavelengths are preference for long-range weather surveillance and operational applications like snow and rain QPE, severe weather monitoring, and fire weather. Clear-air Bragg scattering at S band has also been used to characterize the convective boundary layer depth (e.g., Banghoff et al. 2018). The "medium wavelength" group includes C (4–8 cm) and X (2.5–4 cm) bands, which are more sensitive than S band. However, because larger precipitation particles (e.g., large raindrops, large melting snowflakes, hailstones) can be appreciable fractions or even larger than these wavelengths, resonance scattering effects complicate the physical interpretation of returned signals (e.g., Ryzhkov and Zrnić 2019). Additionally, attenuation is of greater concern. The "short wavelength" group includes Ka (0.75–1.2 cm) and W (0.1–0.75 cm) bands, and often are used for observations of snow, fire weather, light rain and drizzle, and cloud particles (e.g., Kollias et al. 2007). Resonance scattering effects and attenuation can be significant in precipitation.

Ideally, weather radars would provide information about clouds and precipitation at the largest possible range combined with the finest spatial resolution and the highest sampling rate. However, each frequency band is characterized by a combination of physical and technical advantages and constraints that call for trade-off studies and applications. Important considerations are transportability, angular resolution, and attenuation. As discussed above, attenuation depends on the hydrometeor number concentration and composition and size relative to the wavelength; for the same hydrometeors, shorter wavelengths are more attenuated, which limits the effective range of observations. The angular resolution increases with the frequency and the size of the radar antenna aperture. This has direct implications on transportability and spatial resolution. For example, S-band radars require a large aperture (~8.5 m) compared to C- and X-band radars to produce a 1° beam, which makes transportability more challenging. Also, with a 1° beamwidth, the radar beam is 1 km across at a range of 57 km, which translates into limited vertical resolution. Radars operating at C and X bands, and shorter wavelengths can afford smaller apertures because of their smaller wavelength, which allows them to operate on mobile platforms to increase spatial resolution and limit the impact of attenuation. In addition to transportability and detectability of small particles, short wavelengths provide high angular resolution that is suitable to study atmospheric phenomena occurring over fine spatial scales. For example, a 0.3°-beamwidth Ka-band radar has one-tenth of the resolution volume size compared to a 1.0°-beamwidth centimeter-wavelength radar operating with the same range resolution (i.e., bandwidth).

Future PAR systems will need to cover a wide range of radar frequencies to address critical science questions spanning across communities such as transition regimes, e.g., from clouds to precipitation or mixed-phase clouds. PAR systems and applications at long wavelengths

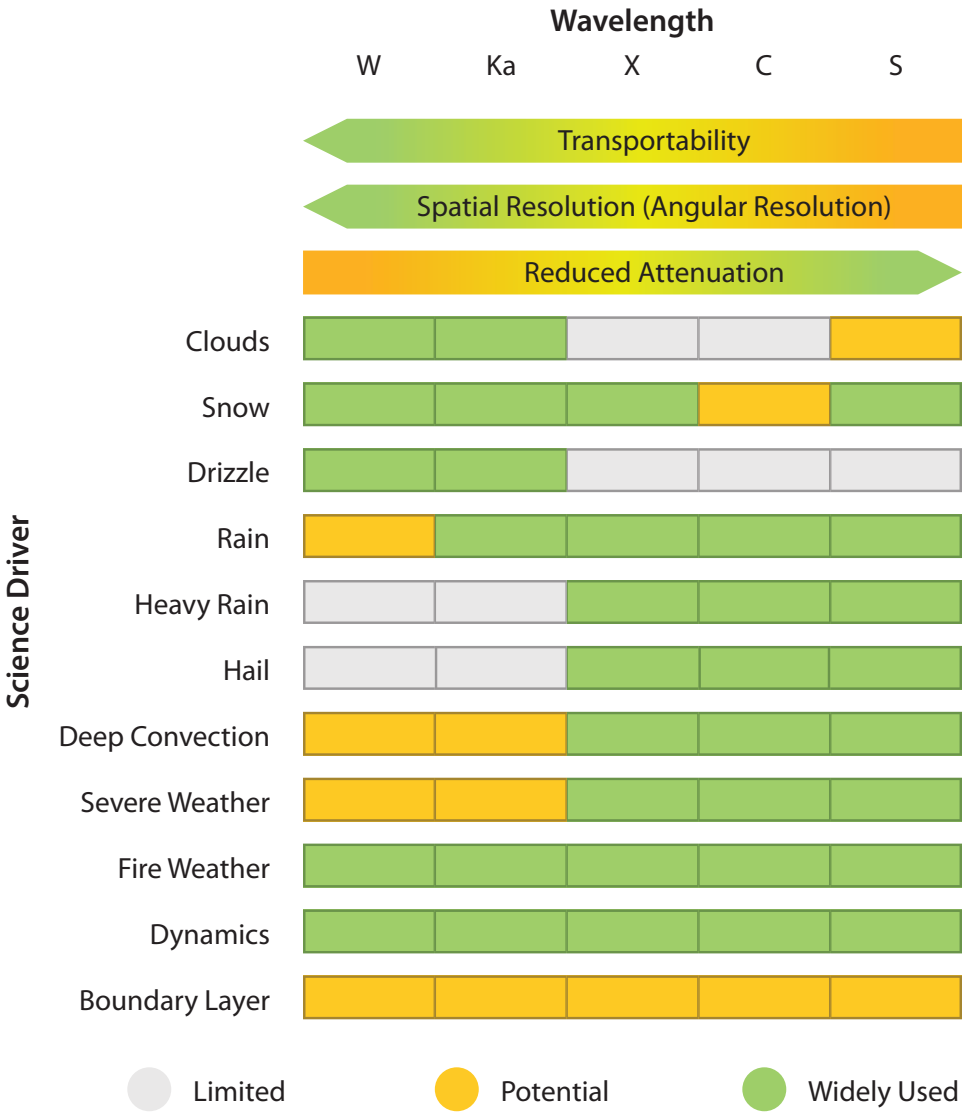

Fig. 8. Summary of applicability of radar wavelengths to specific science drivers.

(S band), medium wavelengths (C, X bands), and short wavelengths (Ka, W bands) are discussed next, with a summary provided in Fig. 8.

PAR system concepts for different science applications.

Long-wavelength applications for long-duration, high-impact weather and climate research. Radar observations have had an indelible impact on the atmospheric sciences through the use of transportable S-band, dual-polarization systems (NCAR S-PolKa; NASA NPOL) supporting National Science Foundation and NASA field campaigns, suborbital research efforts, and NEXRAD's extensive use in basic and operational research. Yet, limitations of mechanically scanning radars lead to an undesirable trade-off between the number of elevation angles and volume scan time, which typically results in sparse vertical coverage at middle and upper levels of the atmosphere.

A notional design for a research S-band PAR is an all-digital, transportable PAR with a 1° beamwidth (Palmer et al. 2022). Since the meteorological community is moving toward a nationwide operational PAR network to replace NEXRAD (Weber et al. 2021), S-band, dual-polarization PAR technology has greater maturity than shorter-wavelength PAR technology. An S-band PAR can serve as a focal point for a field campaign by simultaneously optimizing multiple science missions, such as capturing the microphysical and dynamic processes within several nearby thunderstorms from near the ground to cloud top over

their life cycle, while also obtaining clear-air measurements of the surrounding environment. Although other PAR architectures can perform some degree of adaptive scanning, an all-digital PAR provides the flexibility required to handle multiple scientific missions. Adaptive radar imaging (i.e., adaptive spoiling) and beam multiplexing enable observations of fine spatial scales (several hundreds of meters) and extremely fine temporal scales (tens of seconds) and focusing allows to improve clear-air measurements with longer dwells (e.g., along drylines or outflow boundaries). For instance, the all-digital PAR architecture is uniquely qualified to produce very wide imaging beams in either azimuth or elevation. In contrast, PARs based on analog or subarray beamforming will have limits on the width of the imaging beams, which will limit the degree of adaptive scanning possible to rapidly scan deep and/or widespread storms.

With an all-digital, S-band dual-polarization PAR, the preceding capabilities will enable transformative capabilities for a future operational radar network. Presently, the design of WSR-88D volume coverage patterns is dictated by compromises between sufficient volumetric sampling and revisit times that extend from 5 to 10 min. Different VCPs need to be designed for distinct operational purposes or scientific investigations. For example, forecasters commonly use the Supplemental Adaptive Intra-Volume Low Level Scan (SAILS) mode to increase low-level sampling frequency; however, the volume scan time increases to 7–8 min. With a phased array radar, these undesirable tradeoffs are eliminated by the diversity of scanning strategies that can simultaneously address a wide range of operational needs from the surface (e.g., flood monitoring/forecasting) to echo top heights (for aviation) and increase efficiency across the spectrum of operations. Also, PAR data will be collected volumetrically in 1 min, enabling forecasters to examine rapidly evolving weather signatures for more informed warning operations. For example, continuous sampling in the vertical will enable more detailed depiction of Z_{DR} columns, while simultaneously documenting the near-surface intensification of rotation in developing tornadoes.

Medium-wavelength applications for mobile and transportable systems for high-impact weather. Networks of C- and X-band radars are often deployed during field campaigns for multi-Doppler studies, so it is natural to envision multiple C- and X-band PARs that maintain this capability while revolutionizing scan speeds and flexibility. Although all-digital technology is nascent at S band, sub-array or analog beamforming architectures are more mature at C and X bands. Note that smaller wavelengths make design of an all-digital system more challenging due to less space for electronic components. Moreover, the need for multiple systems likely benefits from a better cost–benefit ratio when using sub-array or analog beamforming at shorter wavelengths.

Mobile C- and X-band dual-polarization PARs could be deployed in small networks to obtain 3D winds and microphysical information on more transient, high-impact phenomena over fine spatial scales (a few hundreds of meters). Mobile radar observations of tornadoes and their parent storms are most commonly made with X-band radars because these provide an acceptable compromise between attenuation and angular resolution. For studies of deep convection and severe storms, networks of C- or X-band PARs could provide critical observations of 3D winds more appropriately matched to the required temporal resolution. Mobile systems could also target warm and cool precipitation processes over complex terrain or enable rapid deployments for studies of wildfires and fast-reacting post-wildfire hydrology processes.

Short-wavelength applications for very high-resolution observations and cloud measurements. Millimeter-wavelength radars (Ka, W band) have enhanced detectability of cloud particles and sample finer spatial scales (tens of meters). Also, improving the understanding of atmospheric boundary layer (ABL) processes is emphasized as a priority to improve weather forecasts and

climate projections National Research Council (1998, 2009). A key limitation of existing short-wavelength radars is 10–15-min volume scan times, which is too long to assume stationarity of cloud and ABL processes. Thus, rapidly collected observations could greatly advance understanding of the dynamics and microphysics of clouds, including capturing the life cycles of shallow cumulus that have lifetimes shorter than 15 min or better constraining processes leading to warm rain formation. These observations could enable improved parameterizations of microphysical processes and radiative transfer in weather and climate models by better constraining both time-rate-of-change measurements and capturing three-dimensional cloud processes.

A key barrier to developing millimeter-wavelength PAR technology is its lack of maturity compared to centimeter wavelengths. With the advancements in Ka-band technology for 5G, there is opportunity to develop PAR systems with simpler PAR architectures. Although highly digitized architectures are more desirable for reconfigurability, the smaller antenna-element spacing poses a unique challenge for fabrication and integration of radar subsystems. One proposed radar concept is called the Ka-band Rapid Volume Imaging Radar (KaRVIR; Salazar et al. 2022), which employs digital beamforming to collect dual-polarization measurements across a 20° field of view, making it possible to collect volume scans in 20 s. A pair of such systems would enable 3D wind measurements not currently possible with scanning systems due to long volume scans.

Applications to broad science agency research. Given the breadth of future applications and the flexibility of PAR technology, the potential exists to impact many science agencies. NSF-supported field campaigns focus on 1–2-month periods and will eventually need small networks of mobile PARs with wavelength diversity. By resolving processes on a finer angular grid and with greater temporal resolution than with current dish radars, PAR technology can also benefit the Department of Energy's Atmospheric Radiation Measurement (ARM) program's goals to advance the understanding of clouds and precipitation processes and their impact on the Earth system. Yet, a challenge is posed in terms of developing short-to-medium wavelength PARs that are reliable enough to provide continuous observations, often in remote locations. More complete vertical scans provided by PAR can support NASA atmospheric science objectives by matching with satellite observations that have high vertical resolution and sampling (Kirstetter et al. 2012; Skofronick-Jackson et al. 2017; National Academies of Science, Engineering, and Medicine 2018). Finally, NOAA is considering a PAR network to replace the WSR-88Ds (McLean et al. 2020), which would enable operational benefits while enabling major advancements in both fundamental and applied research at an unprecedented number of sites nationwide. Cross-agency collaboration and resource sharing on PAR development and usage, as well as improved coordination between the research and operational communities, will be facilitated by PAR's unprecedented flexibility and ability to optimize multiple missions simultaneously.

Vision for PAR's impact on science and education. PARs offer versatile platforms fostering synergy between sensing technologies (e.g., lidars, cameras, satellites) by providing the spatiotemporal continuity desirable to bridge across observations. Vastly expanded depictions and understanding of microphysical, dynamical, and thermodynamical atmospheric processes can be achieved across spatial and temporal scales by combining PAR observations with other instruments. In addition, the flexibility of all-digital PAR architecture allows the easiest path for interfacing with physics-informed artificial intelligence/machine learning (AI/ML) and to optimize concepts of operations for observing different events with a digital-twin simulator. The simulator consists of a standalone local version of the data acquisition and processing software in the actual radar system that uses either simulated or pre-acquired time series IQ data. This enables testing different PAR configurations,

emulating the radar operation and displaying the data under the defined PAR scanning mode for the same precipitation system (Schvartzman and Curtis 2019; Torres and Schvartzman 2020). PAR observations are envisioned to have a critical impact on weather and climate models through data assimilation (DA) experiments and using 4D observations to conduct process-based evaluations of NWP models and improve parameterization schemes Yussouf and Stensrud (2010).

For the success of any new atmospheric sensing technology, broad adoption by the scientific community is imperative. Real-time displays, analysis tools, and ready access to data are key to introducing different user communities (e.g., scientists, students, forecasters) to PAR technology. The breadth of future applications and flexibility of PARs will lead to targeted training and workforce-development opportunities. Once the data are available in a routine manner, new developments will naturally happen across a variety of topical areas including tailored scan strategies, custom waveforms, new data assimilation methodologies, and innovative display frameworks, just to mention a few. Therefore, we believe there is a mandate for the PAR research community to provide open access to these data with the focused purpose of broad adoption that will lead to important benefits to society.

Acknowledgments. The authors thank several sponsors and partners who have played a crucial role in developing PAR technology for atmospheric observations. These include the National Oceanic and Atmospheric Administration, Office of Naval Research, the National Science Foundation, and the University of Oklahoma. This work was partially supported by the NOAA/Office of Oceanic and Atmospheric Research under NOAA–University of Oklahoma Cooperative Agreement NA21OAR4320204, U.S. Department of Commerce. The contributions of Scott Collis through Argonne National Laboratory were supported by the U.S. Department of Energy, Office of Science, Office of Biological and Environmental Research, under Contract DE-AC02-06CH11357. The contributions of Mark Weber and James Kurdzo through MIT Lincoln Laboratory were supported by the United States Air Force under Air Force Contract FA8702-15-D-0001. The contributions of Pavlos Kollias were supported by Contract DE-SC0012704 with the U.S. Department of Energy (DOE) and NSF Grant AGS-2019932. Any opinions, findings, conclusions, or recommendations expressed in this material are those of the authors and do not necessarily reflect the views of the U.S. government.

Data availability statement. Several high-resolution datasets are available at the ARRC data portal https://arrc.ou.edu/data.html, including phased array data. Requests are always encouraged for other archived radar data sets as described on the ARRC data portal. The ARRC's RadarHub visualization platform can be used to view several years of archived mobile radar data (https://radarhub.arrc.ou.edu).

References

Austin, P. M., and S. G. Geotis, 1990: Weather radar at MIT. *Radar in Meteorology*, D. Atlas, Ed., Amer. Meteor. Soc., 22–31, https://doi.org/10.1007/978-1-935704-15-7_4.

Aydell, T. B., and C. B. Clements, 2021: Mobile Ka-band polarimetric Doppler radar observations of wildfire smoke plumes. *Mon. Wea. Rev.*, **149**, 1247–1264, https://doi.org/10.1175/MWR-D-20-0198.1.

Banghoff, J. R., D. J. Stensrud, and M. R. Kumjian, 2018: Convective boundary layer depth estimation from S-band dual-polarization radar. *J. Atmos. Oceanic Technol.*, **35**, 1723–1733, https://doi.org/10.1175/JTECH-D-17-0210.1.

Barton, P., 1980: Digital beam forming for radar. *IEE Proc. F*, **127**, 266–277, https://doi.org/10.1049/ip-f-1.1980.0041.

Biggerstaff, M. I., and Coauthors, 2005: The shared mobile atmospheric research and teaching radar: A collaboration to enhance research and teaching. *Bull. Amer. Meteor. Soc.*, **86**, 1263–1274, https://doi.org/10.1175/BAMS-86-9-1263.

Bluestein, H. B., C. C. Weiss, and A. L. Pazmany, 2003: Mobile Doppler radar observations of a tornado in a supercell near Bassett, Nebraska, on 5 June 1999. Part I: Tornadogenesis. *Mon. Wea. Rev.*, **131**, 2954–2967, https://doi.org/10.1175/1520-0493(2003)131<2954:MDROOA>2.0.CO;2.

——, M. M. French, I. PopStefanija, R. T. Bluth, and J. B. Knorr, 2010: A mobile, phased-array Doppler radar for the study of severe convective storms. *Bull. Amer. Meteor. Soc.*, **91**, 579–600, https://doi.org/10.1175/2009BAMS2914.1.

——, and Coauthors, 2014: Radar in atmospheric sciences and related research: Current systems, emerging technology, and future needs. *Bull. Amer. Meteor. Soc.*, **95**, 1850–1861, https://doi.org/10.1175/BAMS-D-13-00079.1.

Bodine, D. J., M. R. Kumjian, R. D. Palmer, P. L. Heinselman, and A. V. Ryzhkov, 2013: Tornado damage estimation using polarimetric radar. *Wea. Forecasting*, **28**, 139–158, https://doi.org/10.1175/WAF-D-11-00158.1.

Boettcher, J., S. Torres, F. Nai, C. Curtis, and D. Schvartzman, 2022: A multidisciplinary method to support the evolution of NWS weather radar technology. *Wea. Forecasting*, **37**, 429–444, https://doi.org/10.1175/WAF-D-21-0159.1.

Bowden, K. A., and P. L. Heinselman, 2016: A qualitative analysis of NWS forecasters' use of phased-array radar data during severe hail and wind events. *Wea. Forecasting*, **31**, 43–55, https://doi.org/10.1175/WAF-D-15-0089.1.

——, ——, D. M. Kingfield, and R. P. Thomas, 2015a: Impacts of phased-array radar data on forecaster performance during severe hail and wind events. *Wea. Forecasting*, **30**, 389–404, https://doi.org/10.1175/WAF-D-14-00101.1.

——, ——, ——, and ——, 2015b: Impacts of phased-array radar data on forecaster performance during severe hail and wind events. *Wea. Forecasting*, **30**, 389–404, https://doi.org/10.1175/WAF-D-14-00101.1.

Brandes, E. A., 1977: Gust front evolution and tornado genesis as viewed by Doppler radar. *J. Appl. Meteor.*, **16**, 333–338, https://doi.org/10.1175/1520-0450(1977)016<0333:GFEATG>2.0.CO;2.

Bringi, V., and V. Chandrasekar, 2001: *Polarimetric Doppler Weather Radar: Principles and Applications.* Cambridge University Press, 664 pp.

Brookner, E., 2002: Phased array radars-past, present and future. *RADAR2002*, Edinburgh, United Kingdom, IET, 104–113, https://doi.org/10.1109/RADAR.2002.1174663.

Bukovčić, P., A. Ryzhkov, and D. Zrnić, 2020: Polarimetric relations for snow estimation radar verification. *J. Appl. Meteor. Climatol.*, **59**, 991–1009, https://doi.org/10.1175/JAMC-D-19-0140.1.

Byrd, A. D., R. D. Palmer, and C. J. Fulton, 2020: Development of a low-cost multistatic passive weather radar network. *IEEE Trans. Geosci. Remote Sens.*, **58**, 2796–2808, https://doi.org/10.1109/TGRS.2019.2955606.

——, ——, and ——, 2021: Doppler velocity bias mitigation through sidelobe whitening for multistatic weather radar. *IEEE Trans. Geosci. Remote Sens.*, **59**, 1130–1142, https://doi.org/10.1109/TGRS.2020.2997882.

Carlin, J. T., J. Gao, J. C. Snyder, and A. V. Ryzhkov, 2017: Assimilation of Z_{DR} columns for improving the spinup and forecast of convective storms in storm-scale models: Proof-of-concept experiments. *Mon. Wea. Rev.*, **145**, 5033–5057, https://doi.org/10.1175/MWR-D-17-0103.1.

Caya, A., J. Sun, and C. Snyder, 2005: A comparison between the 4DVAR and the ensemble Kalman filter techniques for radar data assimilation. *Mon. Wea. Rev.*, **133**, 3081–3094, https://doi.org/10.1175/MWR3021.1.

Chandrasekar, V., and Coauthors, 2013: The CASA Dallas Fort Worth remote sensing network ICT for urban disaster mitigation. Geophysical Research Abstracts, Vol. 15, Abstract EGU2013-6351, https://meetingorganizer.copernicus.org/EGU2013/EGU2013-6351-1.pdf.

Chrisman, J. N., 2009: Automated volume scan evaluation and termination (AVSET): A Simple technique to achieve faster volume scan updates. *34th Conf. on Radar Meteorology*, Williamsburg, VA, Amer. Meteor. Soc., P4.4, https://ams.confex.com/ams/34Radar/techprogram/paper_155324.htm.

Chryssomallis, M., 2000: Smart antennas. *IEEE Antennas Propag. Mag.*, **42**, 129–136, https://doi.org/10.1109/74.848965.

Crum, T. D., and R. L. Alberty, 1993: The WSR-88D and the WSR-88D operational support facility. *Bull. Amer. Meteor. Soc.*, **74**, 1669–1688, https://doi.org/10.1175/1520-0477(1993)074<1669:TWATWO>2.0.CO;2.

Cunha, L. K., J. A. Smith, M. L. Baeck, and W. F. Krajewski, 2013: An early performance evaluation of the NEXRAD dual-polarization radar rainfall estimates for urban flood applications. *Wea. Forecasting*, **28**, 1478–1497, https://doi.org/10.1175/WAF-D-13-00046.1.

Curtis, C. D., M. Yeary, and J. L. Lake, 2016: Adaptive nullforming to mitigate ground clutter on the National Weather Radar Testbed phased array radar. *IEEE Trans. Geosci. Remote Sens.*, **54**, 1282–1291, https://doi.org/10.1109/TGRS.2015.2477300.

Dahl, N. A., A. Shapiro, C. K. Potvin, A. Theisen, J. G. Gebauer, A. D. Schenkman, and M. Xue, 2019: High-resolution, rapid-scan dual-Doppler retrievals of vertical velocity in a simulated supercell. *J. Atmos. Oceanic Technol.*, **36**, 1477–1500, https://doi.org/10.1175/JTECH-D-18-0211.1.

Delos, P., B. Broughton, and J. Kraft, 2020: Phased array antenna patterns–Part 2: Grating lobes and beam squint. *Analog Dialogue*, Vol. 54, Analog Devices, Inc., Wilmington, MA, 5 pp., https://www.analog.com/en/analog-dialogue/articles/phased-array-antenna-patterns-part2.html.

Doviak, R. J., and D. Zrnić, 2006: *Doppler Radar and Weather Observations.* Dover Publications, Inc., 481 pp.

Emersic, C., P. L. Heinselman, D. R. MacGorman, and E. C. Bruning, 2011: Lightning activity in a hail-producing storm observed with phased-array radar. *Mon. Wea. Rev.*, **139**, 1809–1825, https://doi.org/10.1175/2010MWR3574.1.

Evans, J. E., and D. M. Bernella, 1994: Supporting the deployment of the terminal Doppler weather radar (TDWR). *Lincoln Lab. J.*, **7** (2), 379–398, https://www.ll.mit.edu/sites/default/files/publication/doc/supporting-deployment-terminal-doppler-weather-evans-ja-7196.pdf.

Frasier, S. J., W. Heberling, C. Wolsieffer, and M. Adam, 2018: X-band phased-array polarimetric radar testbed: Status and initial results. *10th European Conf. on Radar in Meteorology and Hydrology*, Ede-Wageningen, Netherlands, Wageningen University, 298, https://doi.org/10.18174/454537.

French, M. M., H. B. Bluestein, I. PopStefanija, C. A. Baldi, and R. T. Bluth, 2013: Reexamining the vertical development of tornadic vortex signatures in supercells. *Mon. Wea. Rev.*, **141**, 4576–4601, https://doi.org/10.1175/MWR-D-12-00315.1.

Fulton, C., M. Yeary, D. Thompson, J. Lake, and A. Mitchell, 2016: Digital phased arrays: Challenges and opportunities. *Proc. IEEE*, **104**, 487–503, https://doi.org/10.1109/JPROC.2015.2501804.

——, and Coauthors, 2017: Cylindrical polarimetric phased array radar: Beamforming and calibration for weather applications. *IEEE Trans. Geosci. Remote Sens.*, **55**, 2827–2841, https://doi.org/10.1109/TGRS.2017.2655023.

Geerts, B., and Coauthors, 2017: The 2015 Plains Elevated Convection at Night field project. *Bull. Amer. Meteor. Soc.*, **98**, 767–786, https://doi.org/10.1175/BAMS-D-15-00257.1.

Hansen, R. C., 2009: *Phased Array Antennas.* 2nd ed. Wiley-Interscience, 580 pp.

Haupt, R. L., and Y. Rahmat-Samii, 2015: Antenna array developments: A perspective on the past, present and future. *IEEE Antennas Propag. Mag.*, **57**, 86–96, https://doi.org/10.1109/MAP.2015.2397154.

Heberling, W., and S. J. Frasier, 2021: On the projection of polarimetric variables observed by a planar phased-array radar at X-band. *IEEE Trans. Geosci. Remote Sens.*, **59**, 3891–3903, https://doi.org/10.1109/TGRS.2020.3023640.

Heinselman, P. L., D. L. Priegnitz, K. L. Manross, T. M. Smith, and R. W. Adams, 2008a: Rapid sampling of severe storms by the National Weather Radar Testbed phased array radar. *Wea. Forecasting*, **23**, 808–824, https://doi.org/10.1175/2008WAF2007071.1.

——, ——, ——, ——, and ——, 2008b: Rapid sampling of severe storms by the National Weather Radar Testbed phased-array radar. *Wea. Forecasting*, **23**, 808–824, https://doi.org/10.1175/2008WAF2007071.1.

——, D. S. LaDue, and H. Lazrus, 2012: Exploring impacts of rapid-scan radar data on NWS warning decisions. *Wea. Forecasting*, **27**, 1031–1044, https://doi.org/10.1175/WAF-D-11-00145.1.

——, ——, D. M. Kingfield, R. Hoffman, and B. MacAloney, 2013: Simulated NWS tornado warning decisions using rapid-scan radar data. *29th Conf. on Environmental Information Processing Technologies*, Austin, TX, Amer. Meteor. Soc., 8.3, https://ams.confex.com/ams/93Annual/webprogram/Paper219547.html.

——, ——, ——, and ——, 2015: Tornado warning decisions using phased-array radar data. *Wea. Forecasting*, **30**, 57–78, https://doi.org/10.1175/WAF-D-14-00042.1.

Herd, J. S., and M. D. Conway, 2016: The evolution to modern phased array architectures. *Proc. IEEE*, **104**, 519–529, https://doi.org/10.1109/JPROC.2015.2494879.

Hildebrand, P. H., W.-C. Lee, C. A. Walther, C. Frush, M. Randall, E. Loew, R. Neitzel, R. Parsons, J. Testud, F. Baudin, and A. LeCornec, 1996: The ELDORA/ASTRAIA Airborne Doppler Weather Radar: High-Resolution Observations from TOGA COARE. *Bull. Amer. Meteor. Soc.,* **77**, 213–232, https://doi.org/10.1175/1520-0477(1996)077<0213:TEADWR>2.0.CO;2.

Hocking, W., J. Röttger, R. Palmer, T. Sato, and P. Chilson, 2016: *Atmospheric Radar: Application and Science of MST Radars in the Earth's Mesosphere, Stratosphere, Troposphere, and Weakly Ionized Regions.* 1st ed. Cambridge University Press, 854 pp.

Houser, J. B., H. B. Bluestein, and J. C. Snyder, 2015: Rapid-scan, polarimetric, Doppler-radar observations of tornadogenesis and tornado dissipation in a tornadic supercell: The "El Reno, Oklahoma" storm of 24 May 2011. *Mon. Wea. Rev.*, **143**, 2685–2710, https://doi.org/10.1175/MWR-D-14-00253.1.

Hudlow, M., R. K. Farnhudsworth, and P. R. Anhert, 1985: NEXRAD technical requirements for precipitation estimation and accompanying economic benefits. Hydro Tech. Note 4, National Weather Service, 49 pp., https://repository.library.noaa.gov/view/noaa/6635.

Isom, B., and Coauthors, 2013: The atmospheric imaging radar: Simultaneous volumetric observations using a phased array weather radar. *J. Atmos. Oceanic Technol.*, **30**, 655–675, https://doi.org/10.1175/JTECH-D-12-00063.1.

Ivić, I. R., 2017: An approach to simulate the effects of antenna patterns on polarimetric variable estimates. *J. Atmos. Oceanic Technol.*, **34**, 1907–1934, https://doi.org/10.1175/JTECH-D-17-0015.1.

——, 2019: A simple hybrid technique to reduce bias of copolar correlation coefficient estimates. *J. Atmos. Oceanic Technol.*, **36**, 1813–1833, https://doi.org/10.1175/JTECH-D-18-0226.1.

——, 2021: On the polarimetric variable improvement via alignment of subarray channels in PPAR using weather returns. *IEEE Trans. Geosci. Remote Sens.*, **59**, 2015–2027, https://doi.org/10.1109/TGRS.2020.3003293.

——, and D. Schvartzman, 2019: A first look at the ATD data corrections. *39th Int. Conf. on Radar Meteorology*, Nara, Japan, Amer. Meteor. Soc., 2-06.

——, and D. Schvartzman, 2020: Weather calibration efforts on the advanced technology demonstrator. *36th Conf. on Environmental Information Processing Technologies*, Boston, MA, Amer. Meteor. Soc., 8B.4, https://ams.confex.com/ams/2020Annual/meetingapp.cgi/Paper/363084.

——, C. Curtis, E. Forren, R. Mendoza, D. Schvartzman, S. Torres, D. Wasielewski, and F. A. Zahrai, 2019: An overview of weather calibration on the advanced technology demonstrator. *IEEE Int. Symp. on Phased Array Systems and Technology*, Waltham, MA, IEEE, 7 pp., https://doi.org/10.1109/PAST43306.2019.9021053.

——, R. Mendoza, D. Schvartzman, S. Torres, and D. Wasielewski, 2020: Preliminary report on polarimetric calibration for the advanced technology demonstrator. NOAA/NSSL Rep., 34 pp., www.nssl.noaa.gov/publications/par_reports/Preliminary%20Report%20on%20Polarimetric%20Calibration%20for%20the%20Advanced%20Technology%20Demonstrator.pdf.

——, M. Conway, S. M. Torres, J. S. Herd, D. S. Zrnić, and M. E. Weber, 2022: Meteorological polarimetric phased array radar. *Polarimetric Radar Signal Processing*, A. Aubry, A. De Maio, and A. Farina, Eds., Institution of Engineering and Technology, in press.

Jung, Y., G. Zhang, and M. Xue, 2008: Assimilation of simulated polarimetric radar data for a convective storm using the ensemble Kalman filter. Part I: Observation operators for reflectivity and polarimetric variables. *Mon. Wea. Rev.*, **136**, 2228–2245, https://doi.org/10.1175/2007MWR2083.1.

——, M. Xue, and G. Zhang, 2010: Simulations of polarimetric radar signatures of a supercell storm using a two-moment bulk microphysics scheme. *J. Appl. Meteor. Climatol.*, **49**, 146–163, https://doi.org/10.1175/2009JAMC2178.1.

Kikuchi, H., E. Yoshikawa, T. Ushio, F. Mizutani, and M. Wada, 2017: Application of adaptive digital beamforming to Osaka University phased array weather radar. *IEEE Trans. Geosci. Remote Sens.*, **55**, 3875–3884, https://doi.org/10.1109/TGRS.2017.2682886.

——, and Coauthors, 2020: Initial observations for precipitation cores with X-band dual polarized phased array weather radar. *IEEE Trans. Geosci. Remote Sens.*, **58**, 3657–3666, https://doi.org/10.1109/TGRS.2019.2959628.

Kirstetter, P.-E., and Coauthors, 2012: Toward a framework for systematic error modeling of spaceborne precipitation radar with NOAA/NSSL ground radar-based national mosaic QPE. *J. Hydrometeor.*, **13**, 1285–1300, https://doi.org/10.1175/JHM-D-11-0139.1.

Kollias, P., E. E. Clothiaux, M. A. Miller, B. A. Albrecht, G. L. Stephens, and T. P. Ackerman, 2007: Millimeter-wavelength radars: New frontier in atmospheric cloud and precipitation research. *Bull. Amer. Meteor. Soc.*, **88**, 1608–1624, https://doi.org/10.1175/BAMS-88-10-1608.

——, D. J. McLaughlin, S. Frasier, M. Oue, E. Luke, and A. Sneddon, 2018: Advances and applications in low-power phased array X-band weather radars. *2018 IEEE Radar Conf.*, IEEE, Oklahoma City, OK, 1359–1364, https://doi.org/10.1109/RADAR.2018.8378762.

——, and Coauthors, 2020: The ARM radar network: At the leading edge of cloud and precipitation observations. *Bull. Amer. Meteor. Soc.*, **101**, E588–E607, https://doi.org/10.1175/BAMS-D-18-0288.1.

——, and Coauthors, 2022: Science applications of phased array radars. *Bull. Amer. Meteor. Soc.*, **103**, E2231–2251, https://doi.org/10.1175/BAMS-D-21-0173.1.

Kumjian, M. R., 2018: Weather radars. *Remote Sensing of Clouds and Precipitation*, C. Andronache, Ed., Springer, 15–63.

——, Z. J. Lebo, and A. M. Ward, 2019: Storms producing large accumulations of small hail. *J. Appl. Meteor. Climatol.*, **58**, 341–364, https://doi.org/10.1175/JAMC-D-18-0073.1.

Kurdzo, J. M., D. J. Bodine, B. L. Cheong, and R. D. Palmer, 2015: High-temporal resolution polarimetric X-band Doppler radar observations of the 20 May 2013 Moore, Oklahoma, tornado. *Mon. Wea. Rev.*, **143**, 2711–2735, https://doi.org/10.1175/MWR-D-14-00357.1.

——, and Coauthors, 2017: Observations of severe local storms and tornadoes with the atmospheric imaging radar. *Bull. Amer. Meteor. Soc.*, **98**, 915–935, https://doi.org/10.1175/BAMS-D-15-00266.1.

Kuster, C. M., J. C. Snyder, T. J. Schuur, T. T. Lindley, P. L. Heinselman, J. C. Furtado, J. W. Brogden, and R. Toomey, 2019: Rapid-update radar observations of Z_{DR} column depth and its use in the warning decision process. *Wea. Forecasting*, **34**, 1173–1188, https://doi.org/10.1175/WAF-D-19-0024.1.

Lake, J. L., M. Yeary, and C. D. Curtis, 2016: Effects of radio frequency interference mitigation strategies on meteorological data. *2016 IEEE Radar Conf.*, Philadelphia, PA, IEEE, 1–5, https://doi.org/10.1109/RADAR.2016.7485155.

Lebrón, R. M., P.-S. Tsai, J. M. Emmett, C. Fulton, and J. L. Salazar-Cerreno, 2020: Validation and testing of initial and in-situ mutual coupling-based calibration

of a dual-polarized active phased array antenna. *IEEE Access*, **8**, 78 315–78 329, https://doi.org/10.1109/ACCESS.2020.2983523.

Lei, L., G. Zhang, and R. J. Doviak, 2013: Bias correction for polarimetric phased-array radar with idealized aperture and patch antenna elements. *IEEE Trans. Geosci. Remote Sens.*, **51**, 473–486, https://doi.org/10.1109/TGRS.2012.2198070.

——, ——, ——, and S. Karimkashi, 2015: Comparison of theoretical biases in estimating polarimetric properties of precipitation with weather radar using parabolic reflector, or planar and cylindrical arrays. *IEEE Trans. Geosci. Remote Sens.*, **53**, 4313–4327, https://doi.org/10.1109/TGRS.2015.2395714.

Li, Z., Y. Zhang, L. Borowska, I. Ivic, D. Mirkovic, S. Perera, G. Zhang, and D. Zrnić, 2021: Polarimetric phased array weather radar data quality evaluation through combined analysis, simulation, and measurements. *IEEE Trans. Geosci. Remote Sens.*, **18**, 1029–1033, https://doi.org/10.1109/LGRS.2020.2990334.

Loeffler, S. D., M. R. Kumjian, M. Jurewicz, and M. M. French, 2020: Differentiating between tornadic and nontornadic supercells using polarimetric radar signatures of hydrometeor size sorting. *Geophys. Res. Lett.*, **47**, e2020GL088242, https://doi.org/10.1029/2020GL088242.

Maese, T., J. Melody, S. Katz, M. Olster, W. Sabin, A. Freedman, and H. Owen, 2001: Dual-use shipborne phased array radar technology and tactical environmental sensing. *Proc. 2001 IEEE Radar Conf.*, Atlanta, GA, IEEE, 7–12, https://doi.org/10.1109/NRC.2001.922942.

Mailloux, R. J., 2017: *Phased Array Antenna Handbook*. 3rd ed. Artech House, 506 pp.

Matrosov, S. Y., K. A. Clark, B. E. Martner, and A. Tokay, 2002: X-band polarimetric radar measurements of rainfall. *J. Appl. Meteor.*, **41**, 941–952, https://doi.org/10.1175/1520-0450(2002)041<0941:XBPRMO>2.0.CO;2.

——, A. V. Ryzhkov, M. Maahn, and G. de Boer, 2020: Hydrometeor shape variability in snowfall as retrieved from polarimetric radar measurements. *J. Appl. Meteor. Climatol.*, **59**, 1503–1517, https://doi.org/10.1175/JAMC-D-20-0052.1.

McIntosh, R. E., S. J. Frasier, and J. B. Mead, 1995: FOPAIR: A focused array imaging radar for ocean remote sensing. *IEEE Trans. Geosci. Remote Sens.*, **33**, 115–124, https://doi.org/10.1109/36.368216.

McLaughlin, D., and Coauthors, 2009: Short-wavelength technology and the potential for distributed networks of small radar systems. *Bull. Amer. Meteor. Soc.*, **90**, 1797–1818, https://doi.org/10.1175/2009BAMS2507.1.

McLean, C. N., L. W. Uccellini, and N. A. Jacobs, 2020: Weather radar follow on plan: Research and risk reduction to inform acquisition decisions. Report to Congress, National Oceanic and Atmospheric Administration, 21 pp., www.nssl.noaa.gov/publications/par_reports/RadarFollowOnPlan_ReporttoCongress_2020June_Final.pdf.

Mead, J. B., G. Hopcraft, S. J. Frasier, B. D. Pollard, C. D. Cherry, D. H. Schaubert, and R. E. McIntosh, 1998: A volume-imaging radar wind profiler for atmospheric boundary layer turbulence studies. *J. Atmos. Oceanic Technol.*, **15**, 849–859, https://doi.org/10.1175/1520-0426(1998)015<0849:AVIRWP>2.0.CO;2.

Mizutani, F., T. Ushio, E. Yoshikawa, S. Shimamura, H. Kikuchi, M. Wada, S. Satoh, and T. Iguchi, 2018: Fast-scanning phased array weather radar with angular imaging technique. *IEEE Trans. Geosci. Remote Sens.*, **56**, 2664–2673, https://doi.org/10.1109/TGRS.2017.2780847.

Nai, F., S. M. Torres, and R. D. Palmer, 2016: Adaptive beamspace processing for phased-array weather radars. *IEEE Trans. Geosci. Remote Sens.*, **54**, 5688–5698, https://doi.org/10.1109/TGRS.2016.2570138.

——, J. Boettcher, C. Curtis, D. Schvartzman, and S. Torres, 2020: The impact of elevation sidelobe contamination on radar data quality for operational interpretation. *J. Appl. Meteor. Climatol.*, **59**, 707–724, https://doi.org/10.1175/JAMC-D-19-0092.1.

National Academies of Science, Engineering, and Medicine, 2018: *Thriving on Our Changing Planet: A Decadal Strategy for Earth Observation from Space.* The National Academies Press, 717 pp.

National Research Council, 1998: *The Atmospheric Sciences: Entering the Twenty-First Century.* The National Academies Press, 373 pp.

——, 2009: *Observing Weather and Climate from the Ground Up: A Nationwide Network of Networks.* The National Academies Press, 250 pp.

Newman, J. F., and P. L. Heinselman, 2012: Evolution of a quasi-linear convective system sampled by phased array radar. *Mon. Wea. Rev.*, **140**, 3467–3486, https://doi.org/10.1175/MWR-D-12-00003.1.

NOAA, 2015: NOAA National Weather Service radar functional requirements. NOAA Tech. Doc., 58 pp., www.roc.noaa.gov/WSR88D/PublicDocs/NOAA_Radar_Functional_Requirements_Final_Sept%202015.pdf.

Ortega, K. L., J. M. Krause, and A. V. Ryzhkov, 2016: Polarimetric radar characteristics of melting hail. Part III: Validation of the algorithm for hail size discrimination. *J. Appl. Meteor. Climatol.*, **55**, 829–848, https://doi.org/10.1175/JAMC-D-15-0203.1.

Oue, M., P. Kollias, A. Ryzhkov, and E. P. Luke, 2018: Toward exploring the synergy between cloud radar polarimetry and Doppler spectral analysis in deep cold precipitating systems in the arctic. *J. Geophys. Res. Atmos.*, **123**, 2797–2815, https://doi.org/10.1002/2017JD027717.

——, ——, S. Y. Matrosov, A. Battaglia, and A. V. Ryzhkov, 2021: Analysis of the microphysical properties of snowfall using scanning polarimetric and vertically pointing multi-frequency Doppler radars. *Atmos. Meas. Tech.*, **14**, 4893–4913, https://doi.org/10.5194/amt-14-4893-2021.

Palmer, R. D., C. J. Fulton, J. Salazar, H. Sigmarsson, and M. Yeary, 2019: The "Horus" radar—An all-digital polarimetric phased array radar for multimission surveillance. *35th Conf. on Environmental Information Processing Technologies*, Phoenix, AZ, Amer. Meteor. Soc., 8A.6, https://ams.confex.com/ams/2019Annual/webprogram/Paper349962.html.

——, and Coauthors, 2022: Transportable phased array radar: Meeting weather community needs. *38th Conf. on Environmental Information Processing Technologies*, Houston, TX, Amer. Meteor. Soc., J4B.2, https://ams.confex.com/ams/102ANNUAL/meetingapp.cgi/Paper/393087.

Park, H. S., A. Ryzhkov, D. Zrnić, and K.-E. Kim, 2009: The hydrometeor classification algorithm for the polarimetric WSR-88D: Description and application to an MCS. *Wea. Forecasting*, **24**, 730–748, https://doi.org/10.1175/2008WAF2222205.1.

Pazmany, A. L., J. B. Mead, H. B. Bluestein, J. C. Snyder, and J. B. Houser, 2013: A mobile, rapid-scanning, X-band, polarimetric (RaXPol) Doppler radar system. *J. Atmos. Oceanic Technol.*, **30**, 1398–1413, https://doi.org/10.1175/JTECH-D-12-00166.1.

Peterson, P. M., N. I. Durlach, W. M. Rabinowitz, and P. M. Zurek, 1987: Multimicrophone adaptive beamforming for interference reduction in hearing aids. *J. Rehabil. Res. Dev.*, **24**, 103–110.

Puzella, A., and R. Alm, 2008: Air-cooled, active transmit/receive panel array. *2008 IEEE Radar Conf.*, Rome, Italy, IEEE, 1–6, https://doi.org/10.1109/RADAR.2008.4720740.

Robinson, S. D., 2002: Utility of tactical environmental processor (TEP) as a Doppler at-sea weather radar. Ph.D. thesis, Naval Postgraduate School, 84 pp.

Roh, W., and Coauthors, 2014: Millimeter-wave beamforming as an enabling technology for 5G cellular communications: Theoretical feasibility and prototype results. *IEEE Commun. Mag.*, **52**, 106–113, https://doi.org/10.1109/MCOM.2014.6736750.

Ryzhkov, A. V., and D. S. Zrnić, 2019: *Radar Polarimetry for Weather Observations.* Springer, 497 pp.

——, T. J. Schuur, D. W. Burgess, and D. S. Zrnić, 2005: Polarimetric tornado detection. *J. Appl. Meteor.*, **44**, 557–570, https://doi.org/10.1175/JAM2235.1.

——, M. R. Kumjian, S. M. Ganson, and A. P. Khain, 2013a: Polarimetric radar characteristics of melting hail. Part I: Theoretical simulations using spectral microphysical modeling. *J. Appl. Meteor. Climatol.*, **52**, 2849–2870, https://doi.org/10.1175/JAMC-D-13-073.1.

——, ——, ——, and P. Zhang, 2013b: Polarimetric radar characteristics of melting hail. Part II: Practical implications. *J. Appl. Meteor. Climatol.*, **52**, 2871–2886, https://doi.org/10.1175/JAMC-D-13-074.1.

Sadhu, B., and Coauthors, 2017: A 28-GHz 32-element TRX phased-array IC with concurrent dual-polarized operation and orthogonal phase and gain control for 5G communications. *IEEE J. Solid-State Circuits*, **52**, 3373–3391, https://doi.org/10.1109/JSSC.2017.2766211.

Salazar, J. L., E. J. Knapp, and D. J. McLaughlin, 2010: Dual-polarization performance of the phase-tilt antenna array in a CASA dense network radar. *2010 IEEE Int. Geoscience and Remote Sensing Symp.*, Honolulu, HI, IEEE, 3470–3473, https://doi.org/10.1109/IGARSS.2010.5650310.

——, and Coauthors, 2019: An ultra-fast scan C-band polarimetric atmospheric imaging radar (PAIR). *2019 IEEE Int. Symp. on Phased Array System Technology (PAST)*, Waltham, MA, IEEE, 1–5, https://doi.org/10.1109/PAST43306.2019.9021042.

——, and Coauthors, 2022: Dual-Doppler 3D mobile Ka-band rapid-scanning volume imaging radar for earth system science. *38th Conf. on Environmental Information Processing Technologies*, Houston, TX, Amer. Meteor. Soc., 8A.2, https://ams.confex.com/ams/102ANNUAL/meetingapp.cgi/Paper/399483.

Schvartzman, D., 2020: Signal processing techniques and concept of operations for polarimetric rotating phased array radar. Ph.D. thesis, University of Oklahoma, 224 pp., https://hdl.handle.net/11244/326580.

——, and C. D. Curtis, 2019: Signal processing and radar characteristics (SPARC) simulator: A flexible dual-polarization weather-radar signal simulation framework based on preexisting radar-variable data. *IEEE J. Sel. Top. Appl. Earth Obs. Remote Sens.*, **12**, 135–150, https://doi.org/10.1109/JSTARS.2018.2885614.

——, S. Torres, and T.-Y. Yu, 2017: Weather radar spatiotemporal saliency: A first look at an information theory–based human attention model adapted to reflectivity images. *J. Atmos. Oceanic Technol.*, **34**, 137–152, https://doi.org/10.1175/JTECH-D-16-0092.1.

——, S. M. Torres, and T.-Y. Yu, 2021a: Motion-compensated steering: Enhanced azimuthal resolution for polarimetric rotating phased array radar. *IEEE Trans. Geosci. Remote Sens.*, **59**, 10073–10093, https://doi.org/10.1109/TGRS.2021.3055033.

——, M. Weber, S. Torres, H. Thomas, D. S. Zrnić, and I. Ivić, 2021b: Scanning concepts and architectures supporting rotating meteorological phased-array radar. *37th Conf. on Environmental Information Processing Technologies*, Online, Amer. Meteor. Soc., 10.8, https://ams.confex.com/ams/101ANNUAL/meetingapp.cgi/Paper/379726.

——, S. Torres, and T. Yu, 2021c: Distributed beams: Concept of operations for polarimetric rotating phased array radar. *IEEE Trans. Geosci. Remote Sens.*, **59**, 9173–9191, https://doi.org/10.1109/TGRS.2020.3047090.

——, R. Palmer, T.-Y. Yu, R. Reinke, and F. Nai, 2022: A pattern synthesis method for polarimetric weather observations with the all-digital horus phased array radar. *38th Conf. on Environmental Information Processing Technologies*, Houston, TX, Amer. Meteor. Soc., 7B.1, https://ams.confex.com/ams/102ANNUAL/meetingapp.cgi/Paper/395979.

Skofronick-Jackson, G., and Coauthors, 2017: The Global Precipitation Measurement (GPM) mission for science and society. *Bull. Amer. Meteor. Soc.*, **98**, 1679–1695, https://doi.org/10.1175/BAMS-D-15-00306.1.

Skoinik, M., 2008: *Radar Handbook*. McGraw-Hill, 846 pp.

Stailey, J. E., and K. D. Hondl, 2016: Multifunction phased array radar for aircraft and weather surveillance. *Proc. IEEE*, **104**, 649–659, https://doi.org/10.1109/JPROC.2015.2491179.

Steyskal, H., 1988: Digital beamforming—An emerging technology. *MILCOM 88: 21st Century Military Communications Conf.– What's Possible?*, San Diego, CA, IEEE, 399–403, https://doi.org/10.1109/MILCOM.1988.13422.

Stout, G. E., and F. A. Huff, 1953: Radar records Illinois tornadogenesis. *Bull. Amer. Meteor. Soc.*, **34**, 281–284, https://doi.org/10.1175/1520-0477-34.6.281.

Talisa, S. H., K. W. O'Haver, T. M. Comberiate, M. D. Sharp, and O. F. Somerlock, 2016: Benefits of digital phased array radars. *Proc. IEEE*, **104**, 530–543, https://doi.org/10.1109/JPROC.2016.2515842.

Tanamachi, R. L., and P. L. Heinselman, 2016: Rapid-scan, polarimetric observations of central Oklahoma severe storms on 31 May 2013. *Wea. Forecasting*, **31**, 19–42, https://doi.org/10.1175/WAF-D-15-0111.1.

Tobin, D. M., and M. R. Kumjian, 2017: Polarimetric radar and surface-based precipitation-type observations of ice pellet to freezing rain transitions. *Wea. Forecasting*, **32**, 2065–2082, https://doi.org/10.1175/WAF-D-17-0054.1.

Tong, M., and M. Xue, 2005: Ensemble Kalman filter assimilation of Doppler radar data with a compressible nonhydrostatic model: OSS experiments. *Mon. Wea. Rev.*, **133**, 1789–1807, https://doi.org/10.1175/MWR2898.1.

Torres, S. M., and D. Schvartzman, 2020: A simulation framework to support the design and evaluation of adaptive scanning for phased-array weather radars. *J. Atmos. Oceanic Technol.*, **37**, 2321–2339, https://doi.org/10.1175/JTECH-D-20-0087.1.

——, and Coauthors, 2016: Adaptive-weather-surveillance and multifunction capabilities of the National Weather Radar Testbed phased array radar. *Proc. IEEE*, **104**, 660–672, https://doi.org/10.1109/JPROC.2015.2484288.

Van Veen, B. D., and K. M. Buckley, 1988: Beamforming: A versatile approach to spatial filtering. *IEEE ASSP Mag.*, **5**, 4–24, https://doi.org/10.1109/53.665.

Vivekanandan, J. W.-C. Lee, E. Loew, J. L. Salazar, V. Grubišić, J. Moore, and P. Tsai, 2014: The next generation airborne polarimetric Doppler weather radar. *Geosci. Instrum. Method. Data Syst*., **3**, 111–126, https://doi.org/10.5194/gi-3-111-2014.

Weber, M., and Coauthors, 2021: Towards the next generation operational meteorological radar. *Bull. Amer. Meteor. Soc.*, **102**, E1357–E1383, https://doi.org/10.1175/BAMS-D-20-0067.1.

Whiton, R. C., P. L. Smith, S. G. Bigler, K. E. Wilk, and A. C. Harbuck, 1998: History of the operational use of weather radar by U.S. Weather Services. Part I: The Pre-NEXRAD era. *Wea. Forecasting*, **13**, 219–243, https://doi.org/10.1175/1520-0434(1998)013<0219:HOOUOW>2.0.CO;2.

Wilson, K. A., P. L. Heinselman, C. M. Kuster, D. M. Kingfield, and Z. Kang, 2017: Forecaster performance and workload: Does radar update time matter? *Wea. Forecasting*, **32**, 253–274, https://doi.org/10.1175/WAF-D-16-0157.1.

Wu, C., L. Liu, X. Liu, G. Li, and C. Chen, 2018: Advances in Chinese dual-polarization and phased-array weather radars: Observational analysis of a supercell in southern China. *J. Atmos. Oceanic Technol.*, **35**, 1785–1806, https://doi.org/10.1175/JTECH-D-17-0078.1.

Wurman, J., D. Dowell, Y. Richardson, P. Markowski, E. Rasmussen, D. Burgess, L. Wicker, and H. Bluestein, 2012: The second verification of the origins of rotation in tornadoes experiment: VORTEX2. *Bull. Amer. Meteor. Soc.*, **93**, 1147–1170, https://doi.org/10.1175/BAMS-D-11-00010.1.

Yeary, M., and Coauthors, 2012: Multichannel receiver design, instrumentation, and first results at the national weather radar testbed. *IEEE Trans. Instrum. Meas.*, **61**, 2022–2033, https://doi.org/10.1109/TIM.2011.2178671.

——, R. Palmer, C. Fulton, J. Salazar, and H. Sigmarsson, 2021: Update on an S-band all-digital mobile phased array radar. *2021 IEEE Radar Conf.*, Atlanta, GA, IEEE, 1–4, https://doi.org/10.1109/RadarConf2147009.2021.9455287.

Yoshida, S., T. Adachi, K. Kusunoki, S. Hayashi, T. Wu, T. Ushio, and E. Yoshikawa, 2017: Relationship between thunderstorm electrification and storm kinetics revealed by phased array radar. *J. Geophys. Res. Atmos.*, **122**, 3821–3836, https://doi.org/10.1002/2016JD025947.

Yoshikawa, E., T. Ushio, Z. Kawasaki, S. Yoshida, T. Morimoto, F. Mizutani, and M. Wada, 2013: MMSE beam forming on fast-scanning phased array weather radar. *IEEE Trans. Geosci. Remote Sens.*, **51**, 3077–3088, https://doi.org/10.1109/TGRS.2012.2211607.

Yu, T.-Y., M. B. Orescanin, C. D. Curtis, D. S. Zrnić, and D. E. Forsyth, 2007: Beam multiplexing using the phased-array weather radar. *J. Atmos. Oceanic Technol.*, **24**, 616–626, https://doi.org/10.1175/JTECH2052.1.

——, M. S. McCord, J. L. Salazar, C. Fulton, R. D. Palmer, and H. Bluestein, 2019: Development of a shared mobile c-band Polarimetric Atmospheric Imaging Radar (PAIR). *39th Int. Conf. on Radar Meteorology*, Nara, Japan, Amer. Meteor. Soc., 2-07.

Yussouf, N., and D. J. Stensrud, 2010: Impact of phased-array radar observations over a short assimilation period: Observing system simulation experiments

using an ensemble Kalman filter. *Mon. Wea. Rev.*, **138**, 517–538, https://doi.org/10.1175/2009MWR2925.1.

Zhang, G., R. J. Doviak, D. S. Zrnić, J. Crain, D. Staiman, and Y. Al-Rashid, 2009: Phased array radar polarimetry for weather sensing: A theoretical formulation for bias corrections. *IEEE Trans. Geosci. Remote Sens.*, **47**, 3679–3689, https://doi.org/10.1109/TGRS.2009.2029332.

——, ——, ——, R. D. Palmer, L. Lei, and Y. Al-Rashid, 2011: Polarimetric phased–array radar for weather measurement: A planar or cylindrical configuration. *J. Atmos. Oceanic Technol.*, **28**, 63–73, https://doi.org/10.1175/2010JTECHA1470.1.

Zhang, J., L. Tang, S. Cocks, P. Zhang, A. Ryzhkov, K. Howard, C. Langston, and B. Kaney, 2020: A dual-polarization radar synthetic QPE for operations. *J. Hydrometeor.*, **21**, 2507–2521, https://doi.org/10.1175/JHM-D-19-0194.1.

Zrnić, D. S., 1987: Three-body scattering produces precipitation signature of special diagnostic value. *Radio Sci.*, **22**, 76–86, https://doi.org/10.1029/RS022i001p00076.

——, and A. V. Ryzhkov, 1999: Polarimetry for weather surveillance radars. *Bull. Amer. Meteor. Soc.*, **80**, 389–406, https://doi.org/10.1175/1520-0477(1999)080⟨0389:PFWSR⟩2.0.CO;2.

——, and Coauthors, 2007: Agile-beam phased array radar for weather observations. *Bull. Amer. Meteor. Soc.*, **88**, 1753–1766, https://doi.org/10.1175/BAMS-88-11-1753.

——, G. Zhang, and R. J. Doviak, 2011: Bias correction and Doppler measurement for polarimetric phased-array radar. *IEEE Trans. Geosci. Remote Sens.*, **49**, 843–853, https://doi.org/10.1109/TGRS.2010.2057436.